Available online at www.sciencedirect.com
ScienceDirect
Geochimica et Cosmochimica Acta 75 (2011) 978–1002
Geochimica et Cosmochimica Acta
www.elsevier.com/locate/gca

Chemical weathering, river geochemistry and atmospheric carbon fluxes from volcanic and ultramafic regions on Luzon Island, the Philippines

H.H. Schopka [a,*], L.A. Derry [a], C.A. Arcilla [b]

[a] Department of Earth and Atmospheric Sciences, Cornell University, Ithaca, NY 14853, USA
[b] National Institute of Geological Sciences, University of the Philippines, Diliman, Quezon City 1101, Philippines

Received 7 April 2010; accepted in revised form 12 November 2010; available online 17 November 2010

Abstract

We investigated rates of chemical weathering of volcanic and ophiolitic rocks on Luzon Island, the Philippines. Luzon has a tropical climate and is volcanically and tectonically very active, all factors that should enhance chemical weathering. Seventy-five rivers and streams (10 draining ophiolites, 65 draining volcanic bedrock) and two volcanic hot springs were sampled and analyzed for major elements, alkalinity and $^{87}Sr/^{86}Sr$. Cationic fluxes from the volcanic basins are dominated by Ca^{2+} and Mg^{2+} and dissolved silica concentrations are high (500–1900 μM). Silica concentrations in streams draining ophiolites are lower (400–900 μM), and the cationic charge is mostly Mg^{2+}. The areally weighted average CO_2 export flux from our study area is $3.89 \pm 0.21 \times 10^6$ mol/km^2/yr, or $5.99 \pm 0.64 \times 10^6$ mol/km^2/yr from ophiolites and $3.58 \pm 0.23 \times 10^6$ mol/km^2/yr from volcanic areas (uncertainty given as ±1 standard error, s.e.). This is ~6–10 times higher than the current best estimate of areally averaged global CO_2 export by basalt chemical weathering and ~2–3 times higher than the current best estimate of CO_2 export by basalt chemical weathering in the tropics. Extrapolating our findings to all tropical arcs, we estimate that around one tenth of all atmospheric carbon exported via silicate weathering to the oceans annually is processed in these environments, which amount to ~1% of the global exorheic drainage area. Chemical weathering of volcanic terranes in the tropics appears to make a disproportionately large impact on the long-term carbon cycle.

1. INTRODUCTION

Weathering of Ca- and Mg-rich silicate rocks and burial of organic carbon are the two main mechanisms responsible for removal of CO_2 from the atmosphere over geological timescales. These processes are counteracted by volcanic degassing of CO_2, oxidation of organic matter and decarbonation of carbonate rocks during metamorphism. Chemical weathering of silicate minerals is mediated by carbonic acid formed as atmospheric CO_2 dissolves in water (or, equivalently, by organic acids derived from soil organic matter). An example is the incongruent dissolution of anorthite, Ca-feldspar:

$$CaAl_2Si_2O_{8(s)} + 2\,CO_{2(g)} + 3\,H_2O = Al_2Si_2O_5\,(OH)_4 + Ca^{2+} + 2\,HCO_3^- \quad (1)$$

The products of the reaction are a clay mineral (kaolinite in this example), dissolved cations and bicarbonate. The bicarbonate and cations formed in the above reaction are transported to the oceans where they may precipitate as carbonates. The net result of the weathering process is the removal of carbon dioxide from the ocean–atmosphere system. The mechanisms that control weathering fluxes on large scales remain incompletely understood. Temperature, rainfall, lithology, basin relief, and erosion rate are among

* Corresponding author.
E-mail address: hhs22@cornell.edu (H.H. Schopka).

0016-7037/$ - see front matter © 2010 Elsevier Ltd. All rights reserved.
doi:10.1016/j.gca.2010.11.014

the variables that have been investigated in an effort to identify the key control mechanisms on global weathering fluxes.

Meybeck (1987) showed that basalt weathers at faster rates than other silicate rocks, such as granitoids and metamorphics. Several studies have confirmed that elevated rates of atmospheric carbon consumption accompany fast weathering rates in basaltic and andesitic regions (Gislason et al., 1996; Louvat and Allegre, 1997; Dessert et al., 2003; Das et al., 2005). Gaillardet et al. (1999), in their study of the CO_2 consumption by rock weathering in the largest river basins in the world, report a correlation between rates of physical and chemical erosion. Milliman and Syvitski (1992) showed that sediment fluxes from high-standing oceanic islands (HSIs) are of the same order of magnitude as sediment fluxes from all the large rivers of the world combined, and went on to demonstrate that the HSI of the East Indies alone (comprising ~2% of global land area) contribute 20–25% of the global sediment export from land to sea (Milliman et al., 1999). These regions have abundant ultramafic to intermediate volcanic rocks, are tectonically active, experience warm and wet climate, and high erosion rates. All of these factors should act to enhance chemical weathering. Work by Lyons et al. (2005) confirmed the high chemical erosion rates associated with rapid physical erosion rates in sedimentary rocks on New Zealand and Goldsmith et al. (2008) reported very high chemical erosion rates in areas of intermediate volcanism in New Zealand. Rad et al. (2006) and Goldsmith et al. (2010) found comparably high chemical weathering rates in watersheds with intermediate lithology on various islands in the Lesser Antilles. We therefore hypothesize that chemical weathering rates, and the associated CO_2 consumption rates, in the volcanic island arcs in tropical regions of Oceania and Central America should be high.

The Philippines (Fig. 1a and b) is an ideal place to investigate the rates of consumption of atmospheric CO_2 by weathering processes in a volcanic arc in a young, tectonically active tropical setting. Oceanic crust is subducted under the archipelago in four different subduction zones (Schellart and Rawlinson, 2010) and earthquakes and volcanic eruptions are consequently very common. Located at between 5 and 20°N, the over 1000 islands that comprise the archipelago lie within the tropical cyclone track in the western Pacific and have an area of just under 300,000 km^2. The climate is hot and humid. We focused our field work on the largest island, Luzon. Since our intent was to investigate controls on chemical weathering rates of mafic and ultramafic rocks we avoided watersheds known to contain significant amounts of carbonate rocks, while including watersheds that cover the entire range of mafic and intermediate lithologies and climate found on Luzon. Several of the watersheds studied are influenced by hydrothermal activity related to volcanism; the weathering component derived from the hydrothermal activity is referred to as high-temperature, or "high-T", weathering (Evans et al., 2001) in the following text, as opposed to low-temperature, or "low-T", weathering proceeding at ambient temperatures.

2. GEOLOGY AND CLIMATE

Most of the streams and rivers studied drain the major currently active volcanic regions on Luzon; the Bataan Volcanic Arc, the Macolod Corridor and the Bicol Volcanic Arc (Figs. 1b, 2 and 3). We also sampled streams draining older volcanic rocks in the Southern Sierra Madre and on the Bicol Peninsula, as well as streams draining ultramafic rocks (ophiolites) in Zambales and Rizal Provinces. The geology of each region is described in the following, geological maps are shown in Fig. 3, and sources are listed where they are discussed. The major element chemistry and Sr-isotope composition of representative volcanic rocks from the study area, collected from published sources, are listed in Tables EA1 and EA2, respectively.

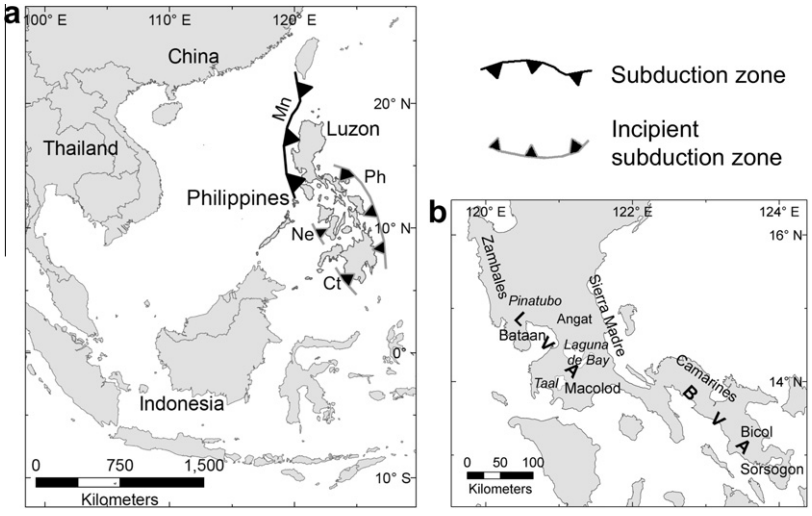

Fig. 1. The Philippines, adjacent land masses and locations referred to in the text. (a) Location of the Philippines in SE Asia. Subduction zones around the Philippines are modified from Schellart and Rawlinson (2010); Mn: Manila, Ne: Negros, Ct: Cotabato and Ph: Philippine Trenches. The dark box denotes the region shown in (b). (b), Names of regions used in text.

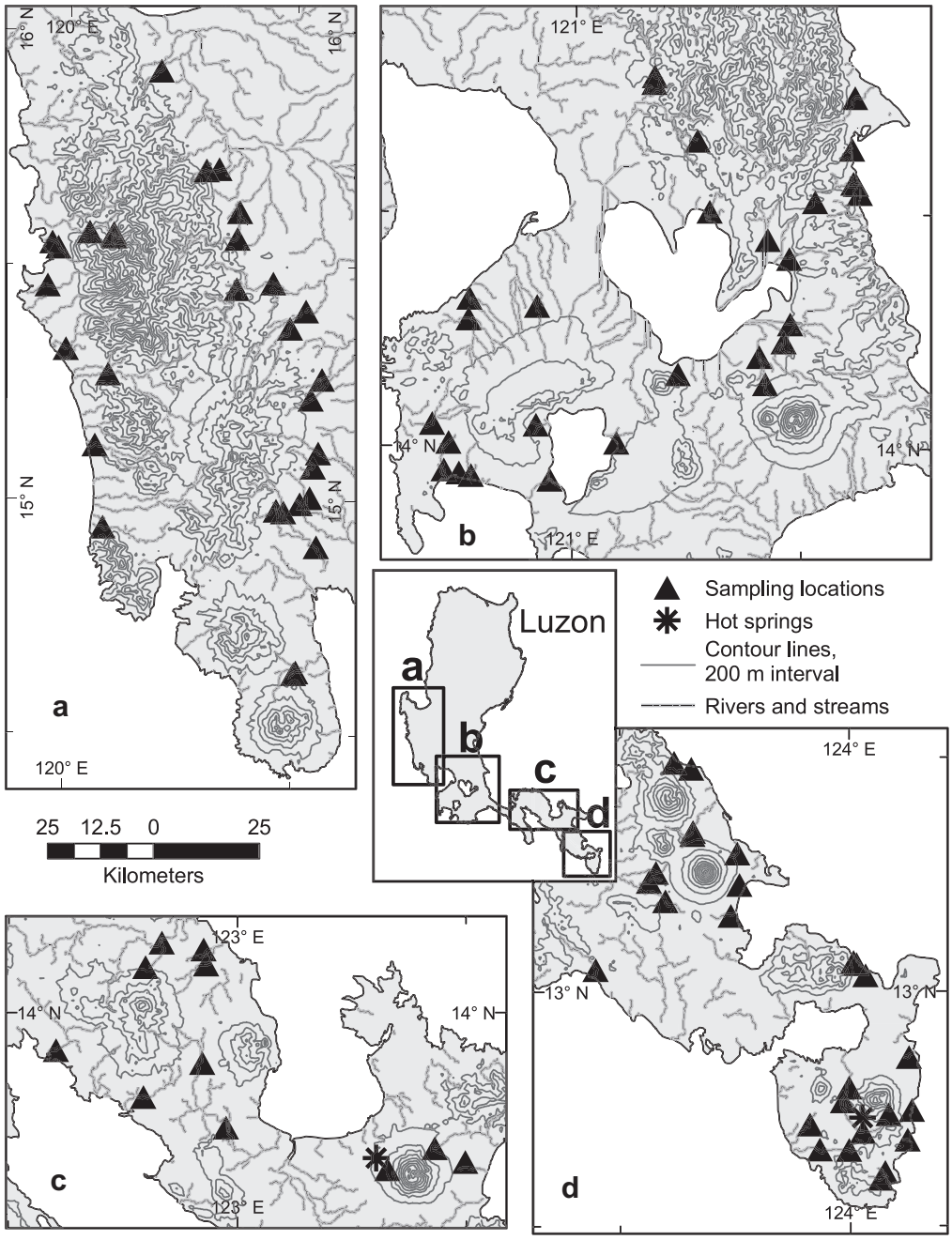

Fig. 2. Sampling locations on Luzon. Thin grey lines are contour lines with 400 m interval; bold grey lines represent main rivers and streams. (a) Sampling locations in the Zambales ophiolite, around Pinatubo and on the Bataan Peninsula. (b) Sampling locations in Taal, the Macolod Corridor, around Laguna de Bay and in the southern Sierra Madre mountains. (c) Sampling locations in the provinces of Camarines Norte and Camarines Sur. (d) Sampling locations in Bicol and Sorsogon provinces.

2.1. Zambales and Angat ophiolites

The Zambales ophiolite (Figs. 2a and 3a) is a supra-subduction-zone ophiolite (Hawkins and Evans, 1983; Evans et al., 1991; Yumul et al., 2000) NW of Manila. It comprises extensive outcrops of peridotite, dunite and gabbro, as well as diabase dike complexes. The rocks of the Zambales ophiolite are altered into various alteration assemblages, from greenschist to amphibolites (Evans et al., 1991). Evans et al. (1991) also noted that the average $^{87}Sr/^{86}Sr$ value of whole rock samples from the Zambales ophiolite (0.70451 ± 0.00084 (2σ) are higher than expected for oceanic crust and attribute this to pervasive alteration by seawater.

The Angat ophiolite (Figs. 2b and 3b) is located NE of Manila. It is an incomplete and structurally dissected ophiolite comprised of gabbros, diabase sheeted dikes, tonalites and pillow basalts (Arcilla et al., 1989). No ultramafic rocks

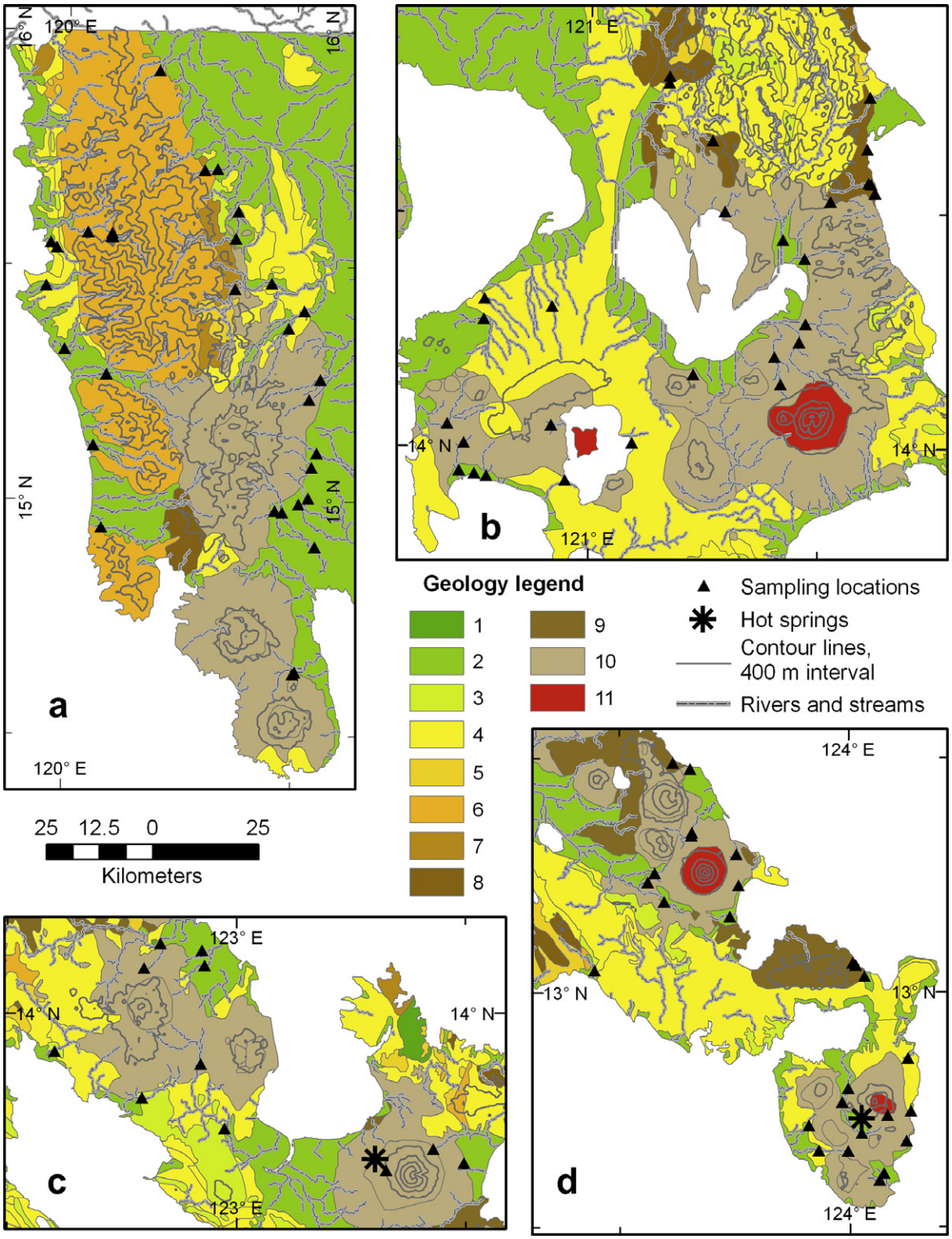

Fig. 3. Geological map of the study areas. The division into parts (a)–(d) is the same as in Fig. 2. Legend: 1 = unknown lithology, 2 = alluvium, recent; 3 = limestone; 4 = sedimentary and metamorphic rocks, undifferentiated; 5 = intrusive rocks, undifferentiated; 6 = ultramafic rocks; 7 = volcanics, undifferentiated; 8 = volcanics, Cretaceous-Eocene; 9 = volcanics, Miocene-Pliocene; 10 = volcanics, Pliocene-Holocene; 11 = volcanics, active. (a) Geology of the Zambales ophiolite and the NW section of the LVA. (b) Geology of the Macolod Corridor (SE section of the LVA and adjacent volcanoes) and the southern Sierra Madre mountains. (c) Geology of Camarines Norte and Camarines Sur provinces, in the NW section of the BVA. (d) Geology of Bicol and Sorsogon provinces in the SE section of the BVA. Modified from the Geological Map of the Philippines published by the Bureau of Mines (Anonymous, 1963).

are exposed. All the rocks have undergone alteration up to greenschist facies and the primary minerals, especially olivine, have been largely replaced by alteration products such as chlorite and amphibole. Encarnación et al. (1993) report zircon U–Pb ages of 45–48 Ma for both the Zambales and Angat ophiolites. There are no $^{87}Sr/^{86}Sr$ data available for the Angat ophiolite but based on the similar age and degree of alteration of the Angat and Zambales ophiolites, we infer that they have similar $^{87}Sr/^{86}Sr$ values.

2.2. Luzon Volcanic Arc

Subduction of the South China Sea plate along the Manila Trench has caused volcanism along the Luzon Arc since the Miocene. This subduction zone is about 1200 km long and stretches from Taiwan through Northern and Central Luzon down to Mindoro (Defant et al., 1989). It comprises six distinct segments, namely Mindoro, Macolod Corridor, Bataan, Northern Luzon, Babuyan and Taiwan. This study included the Bataan (Figs. 2a and b, 3a and b) and the Macolod Corridor (Figs. 2b and 3b) segment of the Luzon Arc. The Bataan segment is an N–S trending arcuate zone that follows the western coast of Luzon from the Gulf of Lingayen south to Central Luzon. This segment gives way to the Macolod Corridor in the immediate vicinity of Lake Taal, where the volcanic trend changes to NE–SW.

Both the Bataan segment and the Macolod Corridor produce high to medium-K calc-alkaline rocks. The Bataan segment consists of two sub-parallel lines of volcanoes. The arc front volcanoes (AFV) are located closer to the shore and thus closer to the trench. Activity in the AFV has been dated at 7–0.2 Myr although volcanism continues there to the present day, most notably at Pinatubo (Pallister et al., 1992) and at Taal Volcano. Four volcanoes comprise the back arc volcanoes, formed between 1.7 and 0.1 Myr (Defant et al., 1989).

The Macolod Corridor is a 40-km wide zone of intense volcanism, comprising two calderas, several stratovolcanoes and hundreds of monogenetic volcanic edifices such as maars and scoria cones. It is interpreted as a pull-apart zone between the Manila Trench and the Philippine Fault, crossing Luzon in a NE–SW direction, perpendicular to the trend of both the remaining segments of the Luzon Volcanic Arc (LVA) and the Bicol Volcanic Arc (Section 2.4) (Förster et al., 1990). Volcanic activity in the Macolod Corridor has migrated from the NE to the SW through time. Explosive activity commenced in the northern part ~2 Myr ago and lasted to 1.36 Myr ago, when the volcanic front started to move to the southwest. Quiescent, monogenetic volcanism dominated until ~0.5 Ma, when the volcanic front had moved to the southwestern part of the area. At that point, explosive eruptions returned and continue to the present day (Ku et al., 2009).

2.3. Southern Sierra Madre

The basement of the Southern Sierra Madre mountain range (Figs. 2b and 3b) consists of volcanic, plutonic and sedimentary rocks, much of them metamorphosed. The sequence is believed to be a volcanic arc/back arc basin pair dating back to late Mesozoic to early Tertiary times. The basement rocks are covered with sedimentary sequences deposited in a marine shelf environment from the late Oligocene to Quaternary times, and more recent terrigenous sediments. This marine sedimentary sequence comprises extensive limestones, tuffaceous and other volcaniclastic sediments, shale, sandstone and conglomerate. Nonmarine volcaniclastic sediments make their first appearance in the Early Pleistocene and are composed mainly of tuffs and welded volcanic breccias (Bachman et al., 1983). No chemistry data or Sr isotope values are available for the rocks in this region, as far as the authors are aware. In the following discussion, streams in the Southern Sierra Madre region are grouped with streams in the LVA.

2.4. Bicol Volcanic Arc

The Bicol Peninsula (Figs. 2c and d, and 3c and d) is the southernmost extension of Luzon. About a dozen volcanic centers are found on the peninsula. Three are currently active (Mayon, Bulusan and Iriga) and three more are considered potentially active (Labo, Isarog and Malinao) (http://www.phivolcs.dost.gov.ph/). Streams draining all of these volcanoes, except for Iriga, were sampled. The peninsula has a basement of ultramafic and metamorphic rocks that are capped with limestone, deep marine sediments and volcanic rocks. Young carbonates and alluvium mantle the low-lying regions of the peninsula (Andal, 2002).

Current volcanism in the Bicol Volcanic Arc (BVA) is related to the subduction of the Philippine Sea Plate along the Philippine Trench under the Philippine Archipelago. The volcanic rocks on the Bicol Peninsula span the range from basalts through basaltic andesites and andesites to dacites and rhyolites. They all belong to the calc-alkaline series, except for Mt. Mayon which is unique among Bicol volcanoes in that it erupts two magma series, arc tholeiite and calk-alkaline (Andal et al., 2005 and references therein). The current subduction regime started 7 Ma ago. Volcanic rocks formed in the current subduction regime show a younging-southward trend that implies that subduction propagated towards the south (Ozawa et al., 2004). Currently, the youngest volcanic rocks in Bicol are found on and around Mt. Mayon and Mt. Bulusan, both of which have been very active in recent decades. The oldest volcanic rocks that have been identified in Bicol to date are 43 Ma and are not considered to have formed as a result of subduction along the Philippine Trench (Ozawa et al., 2004).

2.5. Climate

Temperatures vary very little throughout the area studied. The average annual temperature as measured at 15 weather stations distributed throughout the study area is 27.3 ± 0.8 (2σ) °C. The warmest months are April through June (27–30 °C) and the coolest months are December and January (24–27 °C). Variations in precipitation are considerable across the study region. The western part of the study area (from Zambales east to Taal) shows a strong seasonality in rainfall, with nearly 80% of annual rain falling from June to September and the remainder of the year

being quite dry. In Quezon and on the Bicol peninsula, around 45% of the annual rainfall occurs from October through December and the remaining 55% of annual rainfall is fairly evenly distributed through the remainder of the year. The average total annual precipitation is significantly ($p = 0.03$) higher in the eastern part of the study area than in the west, or 3344 ± 1020 ($\pm 2\sigma$) mm/yr vs. 2446 ± 1704 mm/yr. Both temperature and precipitation data were extracted from the NOAA GHCN-Monthly V2 dataset, accessed at http://bonnet19.cs.qc.edu:7778/pls/rschdata/rd_start.main in February 2009.

3. METHODS

3.1. Fieldwork

We conducted stream sampling in January and February of 2007 and 2008. This corresponds with the dry period in W-Luzon and the end of the wet period in the Bicol Peninsula. Discharge data was collected in the field at the time of sampling using an FP111 Global Water flow probe. A cross-section was measured across the stream and discharge measured at regular intervals along the transect. At water depths of <20 cm, the flow meter was moved slowly up and down through the water column for approximately one minute to get an averaged flow rate. Where the water was deeper than ~20 cm, discharge was measured at discreet intervals up the water column at each station, and the results averaged. Long-term discharge data for some of the streams was obtained from the Department of Hydraulics at the University of the Philippines, Diliman (Section 3.3).

During sampling, pH and temperature of the water was measured *in situ* using a Beckman–Coulter portable pH/T meter. Samples were collected from a fast-flowing section of the stream into plastic syringes that were rinsed 3–4 times in the stream water prior to sample collection. The samples were hand filtered through 0.2 μm nitrate-cellulose filters into acid-washed LDPE bottles. Usually we collected 2 bottles of 125 mL each, with little to no airspace. The samples were kept in cold, dark conditions until arrival at Cornell University. Upon arrival there, one of the bottles for each sample was acidified with ultrapure HNO_3 to a pH of ~2 and all the samples were kept refrigerated.

In total, 105 samples were collected from 75 river basins and 2 hot springs. Table 1 shows the names and locations of the streams studied. Several rivers were sampled twice. The hot spring data were used to estimate hydrothermal inputs to streams. Four river samples are excluded from analysis. These samples show significant seawater contamination (TDS > 1000 mg/L) and are labeled such in Tables 1 and 2.

3.2. Laboratory analyses

For all samples collected in 2007, major cations (Na^+, K^+, Ca^{2+} and Mg^{2+}) were analyzed at Cornell University on a Dionex ICS-2000. Cations (Na^+, K^+, Ca^{2+}, Mg^{2+} and Sr^{2+}) in samples collected in 2008, and Sr^{2+} in samples from 2007, were analyzed using a Jobin Yvon Ultima ICP-AES at Boston University. Precision in cation analyses was generally better than 6%. Anions in all samples were measured at Cornell University on a Dionex ICS-2000 ion chromatograph with a precision better than 5%. Alkalinity was measured by Gran titration, with a precision better than 2%. Dissolved Si was measured at Cornell University using the molybdate blue method (Mortlock and Froelich, 1989) with a precision better than 2%. Sr isotope values were measured using a VG 54 multicollector thermal ionization mass spectrometer (TIMS) at Cornell University with an average error of 0.01%. Repeat measurements of the NBS987 standard give $^{87}Sr/^{86}Sr$ of 0.71025 ± 0.00001. Repeat analyses of the M178 standard from the USGS indicate that the accuracy of our methods is better than 6% for anions, 5% for cations (9% for Na) and 3% for Si. Major element data are presented in Table 2 and Sr isotope data in Table 3.

In nine out of every ten samples collected in 2007 the normalized inorganic charge balance or NICB ($(TZ^+ - TZ^-)/(TZ^+) \times 100$) ranges between −10% and 10%. In samples collected in 2008, NICB is lower than −20% in 16% of cases and −20% to −10% in 41% of cases. It is not clear what causes the large NICB in the 2008 sample batch; (1) both the elemental analysis and alkalinity titrations were repeated in an effort to identify sources of error, (2) the samples from 2008 are from either from the same streams as the 2007 samples or from streams that are very similar to the 2007 streams in terms of watershed characteristics, and (3) the samples from the two different field campaigns received the same post-collection treatment. Our best guess is that this discrepancy is linked to the different instruments used to analyze cations, i.e., that the ICP-OES systematically yields low values relative to the ion chromatograph. Systematic differences between calculated and titrated alkalinity in river waters have also been reported by Wolff-Boenisch et al. (2009). For the majority of our samples we used the Gran alkalinity values in flux calculations (see Table 2). In samples from 2008 where NICB <−10% (i.e., in samples where satisfactory charge balance was not achieved using the Gran alkalinity for HCO_3^-) we used the calculated alkalinity for HCO_3^- instead. The sole exception was sample PH-08-63 where the calculated alkalinity was negative.

3.3. Hydrology

Calculations of chemical fluxes are strongly dependent on hydrological data such as river discharge. Historical and/or recent discharge data are available for a number of rivers in the regions under study here ($n = 55$, see below). Nevertheless, no discharge data are available for most of the rivers that we sampled ($n = 54$, or 72% of the streams sampled). A common strategy to estimate river discharge in studies comparable to ours, where the focus is on chemistry rather than on hydrology and where hydrology data is sparse, is to use the average reported runoff (discharge normalized to watershed area) for a region to calculate discharge of individual streams. We sought to improve predicted runoff by using spatial statistics on simple landscape metrics. We used a 90-m resolution digital elevation model (DEM) obtained from CGIAR-CSI (http://srtm.csi.cgiar.org/) to define watersheds for the streams and rivers studied and to calculate their area. This dataset

Table 1
Sampling locations in Luzon, 2007 and 2008.

Location name	Type	Region	Sample ID	Longitude	Latitude	m a.sl.	Basin elevation, maximum (m a.s.l.)	Basin elevation, average (m a.s.l.)	Basin relief (m)	Area (km^2)	Average annual discharge, 10^6 m^3/yr
Rivers											
Angat ophiolite, region ZA[b]											
Hanginan River	Main	ZA[b]	PH-07-01	121.173	14.779	80	643	309	564	10	25
Lacotan River	Main	ZA	PH-07-02	121.174	14.794	142	773	394	644	7	19
Zambales ophiolite, region ZA[b]											
Alasa River	Main	ZA	PH-08-04	119.955	15.456	14	2034	537	2026	80	203
Bancal River	Main	ZA	PH-08-03[e]	119.999	15.310	6	1786	631	1782	134	86
Bulsa River, us	Tributary	ZA	PH-08-62	120.450	15.465	90	1613	464	1529	295	749
Bulsa River, ds	Main	ZA	PH-07-34	120.370	15.452	123	1613	530	1493	442	1122
Mababo River	Tributary	ZA	PH-07-39, PH-07-40	120.300	15.704	136	1559	798	1428	27	68
Cabarabuan River	Main	ZA	PH-07-36	120.329	15.708	72	1559	663	1503	38	97
Camiling River, us	Tributary	ZA	PH-07-35	120.370	15.559	91	1764	773	1677	256	650
Camiling River, ds	Main	ZA	PH-08-61	120.375	15.616	45	1764	677	1724	298	757
Dumloc River	Main	ZA	PH-07-37	120.199	15.916	23	781	332	758	38	97
Lawis River, us[a]	Tributary	ZA	PH-08-05	120.100	15.560	167	2009	1033	1847	115	292
Lawis Tributary I	Tributary	ZA	PH-08-06	120.100	15.562	157	1759	875	1600	21	53
Lawis River, ds[a]	Main	ZA	PH-07-04, PH-07-33	120.099	15.569	165	2009	999	1861	138	350
Lawis Tributary II	Main	ZA	PH-08-07	120.045	15.571	100	1149	650	1049	8	21
Masinloc River	Main	ZA	PH-07-05, PH-08-08[e]	119.977	15.538	14	1301	461	1288	40	101
Bicol Volcanic Arc, region Bicol											
Bulawan River	Main	Bicol	PH-07-16	123.755	13.296	95	2382	621	2289	17	36
Dobgon River	Main	Bicol	PH-08-40	123.578	13.256	87	2445	495	2358	38	80
Guinobatan River	Main	Bicol	PH-08-38	123.599	13.195	73	2379	261	2307	65	137
Joroel River	Main	Bicol	PH-08-44	123.618	13.491	20	989	402	971	10	21
Kinastillohan River	Main	Bicol	PH-07-24	123.658	13.336	103	1242	445	1153	4	9
Naga River	Main	Bicol	PH-08-42	123.656	13.478	2	139	46	132	14	30
Naga River Tributary	Main	Bicol	PH-08-43	123.656	13.478	2	1398	492	1387	8	17
Paulog River	Main	Bicol	PH-08-21	123.563	13.237	67	1271	220	1210	29	61
Pio Duran River	Main	Bicol	PH-08-39	123.446	13.048	14	504	174	495	66	138
Quinale River	Main	Bicol	PH-08-41	123.659	13.342	64	1920	426	1860	86	180
Santo Domingo River	Main	Bicol	PH-07-19	123.760	13.229	58	2414	672	2361	8	17
Yawa River	Main	Bicol	PH-07-15	123.741	13.163	12	2406	269	2397	57	119
Bicol Volcanic Arc, region Camarines											
Daet River	Main	Camarines	PH-08-47	122.932	14.103	14	1490	302	1481	69	146
Inarihan River	Main	Camarines	PH-07-11	123.327	13.666	399	874	574	489	1.4	3
Kilbay River	Main	Camarines	PH-08-19[e]	122.603	13.920	6	968	168	964	331	326
Matogdon Tributary	Tributary	Camarines	PH-07-26	122.799	14.098	168	324	222	165	2	4
Matogdon River	Main	Camarines	PH-08-49	122.835	14.150	14	1329	306	1319	28	58
Pinaglabanan River	Main	Camarines	PH-08-45	123.430	13.710	166	1916	639	1750	12	26

Ragay River	Main	Camarines	PH-08-20	122.794	13.820	11	975	204	971	120	252
Rangas River	Main	Camarines	PH-07-13	123.497	13.681	69	1983	808	1919	18	38
San Vincente River	Main	Camarines	PH-08-48	122.926	14.135	10	19	13	11	1.3	3
Pulantuna River	Tributary	Camarines	PH-08-46	122.923	13.893	62	1495	306	1446	189	398
Sipocot River	Main	Camarines	PH-07-25	122.975	13.755	16	1495	199	1486	487	1025
Bicol Volcanic Arc, region Sorsogon											
Bacolod River	Main	Sorsogon	PH-08-23	123.997	12.796	25	1500	379	1483	10	22
Bacon River	Main	Sorsogon	PH-08-37	124.034	13.035	15	1030	373	1017	12	25
Bangon River	Main	Sorsogon	PH-08-30	124.075	12.615	9	624	150	619	24	50
Barcelona River	Main	Sorsogon	PH-08-34	124.128	12.861	16	1176	148	1169	27	56
Karangan Stream	Tributary	Sorsogon	PH-07-23	124.083	12.738	282	630	423	352	1.1	2
Cadacan River, us	Tributary	Sorsogon	PH-08-27	124.027	12.701	41	1520	346	1488	34	71
Cadacan River, ds	Main	Sorsogon	PH-07-20	123.984	12.767	58	1520	212	1503	125	263
Pawa River	Main	Sorsogon	PH-08-29	124.066	12.601	14	581	187	575	26	55
San Bartolome River	Main	Sorsogon	PH-08-32	124.124	12.684	7	599	222	597	17	36
San Francisco River	Main	Sorsogon	PH-08-24	123.912	12.718	31	791	160	769	23	49
San Juan Stream	Main	Sorsogon	PH-08-35	124.014	13.059	39	908	323	875	5	10
San Juan II Stream	Main	Sorsogon	PH-08-36	124.008	13.064	91	363	235	288	0.8	2
Solinao River	Tributary	Sorsogon	PH-08-28	123.997	12.662	35	413	165	378	17	37
San Ramon (Magsaysay) River	Main	Sorsogon	PH-08-25	123.933	12.664	21	413	127	401	53	111
Unnamed waterfall	Main	Sorsogon	PH-08-33	124.134	12.748	12	109	70	97	0.2	0
Luzon Volcanic Arc, region BLM[c]											
Balanac River	Main	BLM	PH-08-55	121.460	14.227	12	2158	451	2147	160	337
Buso-Buso River	Main	BLM	PH-08-50	121.268	14.657	211	940	404	738	18	39
Catmon River	Tributary	BLM[c]	PH-07-08	120.504	14.631	45	1038	316	1004	18	39
Diwa River	Main	BLM	PH-07-09	120.508	14.635	29	1403	379	1375	94	198
Pagsanjan River	Main	BLM	PH-07-32	121.473	14.266	35	533	325	522	207	437
Pangil River	Main	BLM	PH-08-54	121.471	14.405	9	529	348	520	53	111
San Antonio River	Main	BLM	PH-08-52	121.423	14.445	8	405	102	398	13	27
Santa Cruz River, us	Tributary	BLM	PH-07-31	121.419	14.138	196	2139	816	1953	22	47
Santa Cruz River, ds	Main	BLM	PH-08-56	121.406	14.196	46	2139	460	2095	107	226
Tanay River	Main	BLM	PH-08-51	121.296	14.505	14	648	309	637	44	92
Luzon Volcanic Arc, region Pinatubo[d]											
Bamban River	Main	Pinatubo	PH-08-65	120.560	15.261	89	1084	345	1000	88	186
Bucao River	Main	Pinatubo	PH-07-06, PH-08-02	120.088	15.279	33	1668	419	1640	557	1173
Gumain River, us	Tributary	Pinatubo	PH-08-71	120.478	14.977	38	n.a.	n.a.	n.a.	127	268
Caulaman River	Tributary	Pinatubo	PH-08-72	120.461	14.981	42	957	320	923	49	103
Gumain River, ds	Main	Pinatubo	PH-08-74	120.569	14.917	7	1568	357	1561	255	536
Maloma River	Main	Pinatubo[d]	PH-07-03, PH-08-01	120.062	15.117	8	1020	275	1013	153	322
Bangot River	Tributary	Pinatubo	PH-08-64	120.488	15.369	103	1464	337	1364	96	203
O'Donnell River	Main	Pinatubo	PH-08-63	120.523	15.406	87	1464	354	1381	279	587
Pasig River	Main	Pinatubo	PH-08-67	120.553	15.103	112	1457	649	1348	56	118
Porac River us	Tributary	Pinatubo	PH-08-68	120.542	15.073	75	1117	361	1046	42	89

(*continued on next page*)

Table 1 (*continued*)

Location name	Type	Region	Sample ID	Longitude	Latitude	m a.sl.	Basin elevation, maximum (m a.s.l.)	Basin elevation, average (m a.s.l.)	Basin relief (m)	Area (km^2)	Average annual discharge, 10^6 m^3/yr
Porac River ds	Main	Pinatubo	PH-08-73	120.535	15.008	35	1117	274	1090	120	252
Sacobia River	Main	Pinatubo	PH-08-66	120.536	15.218	147	972	396	830	33	70
Santol River	Main	Pinatubo	PH-08-70	120.513	14.994	34	214	72	184	18	39
Tabang River	Main	Pinatubo	PH-07-07	120.081	14.942	15	999	140	992	167	425
Luzon Volcanic Arc, region Quezon											
Agus River	Main	Quezon	PH-07-44, PH-08-58	121.608	14.750	47	1510	501	1501	931	1961
Balabag River	Main	Quezon	PH-07-43, PH-08-60	121.625	14.545	25	411	231	403	3	7
Kiloloram River	Main	Quezon	PH-08-57	121.607	14.640	7	295	133	291	0.5	1
Llabak River	Main	Quezon	PH-07-41	121.526	14.527	331	686	481	356	6	13
Tignoan River	Main	Quezon	PH-07-42, PH-08-59;	121.610	14.567	35	1030	361	1013	87	184
Luzon Volcanic Arc, region Taal											
Obispo Stream	Tributary	Taal	PH-08-13	120.728	14.010	56	723	206	668	19	40
Balayan River	Main	Taal	PH-08-14	120.718	13.950	14	723	126	713	82	173
Dacanlao River	Main	Taal	PH-08-17	120.778	13.939	15	766	283	755	56	118
Langgangan River	Main	Taal	PH-08-15	120.751	13.944	16	47	29	31	0.5	1
Laurel River	Main	Taal	PH-07-29	120.919	14.048	26	638	313	619	32	67
Mabacao River	Main	Taal	PH-08-11	120.770	14.273	32	665	299	643	244	514
Mangapol River	Main	Taal	PH-08-09	120.920	14.301	116	671	379	563	39	82
Naic River	Main	Taal	PH-08-10	120.771	14.317	16	664	218	651	77	162
Palico River	Main	Taal	PH-08-12	120.693	14.049	23	713	238	692	161	338
Palsara River	Main	Taal	PH-07-30	121.096	14.011	11	379	280	352	15	31
Pansipit River	Main	Taal	PH-08-18[e]	120.950	13.931	8	936	126	936	624	1314
Pele River	Main	Taal	PH-07-28	121.228	14.157	134	1074	516	950	2	4
Hot springs											
Bicol Volcanic Arc											
Inarihan hot spring		Camarines	PH-07-12	123.321	13.671	331					
San Benon hot spring		Sorsogon	PH-07-22	124.026	12.731	53					

[a] ds = downstream, us = upstream.
[b] ZA = Zambales and Angat.
[c] BLM = Bataan, Laguna and Macolod.
[d] Pinatubo = comprises both streams draining exclusively Pinatubo and streams draining both Pinatubo and the adjacent Zambales ophiolite.
[e] Sample not included in flux analysis due to possible seawater contamination.

Table 2
Major element chemistry of Luzon rivers, 2007 and 2008.

Sample ID	Date	Discharge at sampling (m^3/sec)	T (°C)	pH	F (μmol/L)	Cl (μmol/L)	SO_4 (μmol/L)	Br (μmol/L)	NO_3 (μmol/L)	PO_4 (μmol/L)	Na (μmol/L)	K (μmol/L)	Mg (μmol/L)	Ca (μmol/L)	Si (μmol/L)	Alk (μeq/L)	Alk type[a]	TDS[b] (ppm)
PH-07-01	1/11/07	0.3	29.0	8.23	4	201	98	n.d.	n.d.	n.d.	478	3	559	769	724	2610	a	275
PH-07-02	1/11/07	0.3	26.1	7.71	2	31	64	n.d.	n.d.	n.d.	284	3	610	702	802	2724	a	271
PH-07-03	1/12/07	0.9	30.4	8.13	4	61	111	n.d.	n.d.	n.d.	330	45	963	321	912	2574	a	270
PH-07-04	1/13/07	4.6	23.2	8.31	n.d.[e]	30	23	n.d.	3	n.d.	62	2	769	94	434	1523	a	146
PH-07-05	1/13/07	0.7	29.9	7.65	n.d.	39	44	n.d.	2	n.d.	114	6	999	277	614	2542	b	236
PH-07-06	1/13/07	2.5	29.0	8.34	11	337	2196	n.d.	n.d.	0.7	1499	104	1043	1861	928	2544	a	573
PH-07-07	1/14/07	2.2	25.8	8.06	5	211	895	n.d.	n.d.	2.1	693	98	684	666	1220	1389	a	315
PH-07-08	1/14/07	0.8	27.4	7.36	3	77	32	n.d.	n.d.	n.d.	306	37	229	336	951	1275	a	168
PH-07-09	1/14/07	1.5	27.2	7.47	3	123	90	n.d.	9	1.5	437	58	222	377	989	1334	a	187
PH-07-11	1/17/07	1.3	22.1	7.58	2	66	14	n.d.	n.d.	n.d.	263	64	47	154	1027	629	a	120
PH-07-12[c]	1/17/07		36.8	6.13	13	756	4761	n.d.	n.d.	n.d.	5400	395	4129	3566	2215	10,755	a	1657
PH-07-13	1/17/07	0.8	30.5	5.14	8	115	2025	n.d.	7	n.d.	375	57	235	1592	919	13	a	336
PH-07-15	1/18/07	2.8	30.3	7.80	13	521	1355	n.d.	30	n.d.	1609	156	1275	924	1055	2795	a	496
PH-07-16	1/18/07	2.8	26.4	7.91	12	109	75	n.d.	n.d.	1.3	424	84	152	324	1118	1191	a	181
PH-07-19	1/18/07	0.8	25.7	7.62	13	112	88	n.d.	11	2.7	557	98	216	392	1202	1521	a	216
PH-07-20	1/19/07	40.4	27.9	7.04	8	527	624	n.d.	18	n.d.	1041	123	751	795	1340	2403	a	386
PH-07-22[c]	1/19/07		43.4	6.46	18	2238	3260	3	23	n.d.	4669	266	3610	2305	2203	7792	a	1300
PH-07-23	1/19/07	1.4	23.2	7.51	23	141	124	n.d.	2	1.7	313	49	98	282	997	705	a	143
PH-07-24	1/20/07	0.7	28.1	7.92	9	102	43	n.d.	18	1.9	403	98	140	311	991	1177	a	170
PH-07-25	1/20/07	56.0	27.9	7.48	3	146	34	n.d.	n.d.	n.d.	291	30	176	374	468	1196	a	137
PH-07-26	1/21/07	0.1	24.6	6.87	n.d.	106	22	n.d.	4	n.d.	265	40	77	127	717	557	a	98
PH-07-28	1/30/07	0.0	22.2	7.95	9	147	147	n.d.	19	2.0	343	82	153	252	1192	849	a	169
PH-07-29	1/30/07	0.5	27.1	8.12	27	166	241	n.d.	82	3.5	999	242	521	794	1545	3035	a	390
PH-07-30	1/30/07	0.1	26.1	8.15	17	172	197	n.d.	136	4.1	1637	376	737	1348	1257	5477	a	568
PH-07-31	1/31/07	2.6	23.1	7.60	9	85	41	n.d.	99	6.8	344	103	192	241	1154	1025	a	172
PH-07-32	1/31/07	2.1	22.9	7.40	5	115	27	n.d.	3	0.8	294	47	153	298	626	1043	a	133
PH-07-33	1/29/07		23.2	8.69	n.d.	39	31	n.d.	4	n.d.	55	2	833	63	390	1665	a	154
PH-07-34	2/1/07	2.5	27.5	8.60	3	41	118	n.d.	n.d.	n.d.	358	10	612	500	632	2340	a	237
PH-07-35	2/2/07	1.2	23.0	8.20	n.d.	33	51	n.d.	n.d.	n.d.	213	5	842	460	603	2669	a	249
PH-07-36	2/2/07	0.2	24.6	8.30	4	40	57	n.d.	n.d.	n.d.	203	7	792	546	552	2737	a	253
PH-07-37	2/2/07	0.1	29.9	7.80	n.d.	50	73	n.d.	10	n.d.	294	5	1000	698	885	3445	a	332
PH-07-39	3/5/07			8.40	n.d.	29	43	n.d.	2	n.d.	206	4	837	589	605	2887	a	267
PH-07-40	3/5/07			8.56	n.d.	23	43	n.d.	n.d.	n.d.	191	3	842	581	614	2906	a	267
PH-07-41	3/11/07	0.8	24.0	7.50	n.d.	108	16	n.d.	9	0.9	215	23	106	150	495	572	a	85
PH-07-42	3/11/07	3.3	27.0	8.20	n.d.	133	34	n.d.	2	n.d.	320	10	264	469	655	1576	a	177
PH-07-43	3/11/07	0.4	26.0	7.90	3	148	50	n.d.	2	n.d.	355	19	180	508	691	1489	a	176
PH-07-44	3/11/07	0.8	28.0	7.40	2	129	28	n.d.	2	n.d.	252	7	165	327	488	1021	a	122
PH-08-01	1/24/08	1.5	35.6	8.07	n.d.	67	154	n.d.	0	n.d.	264	53	871	345	908	2395	a	261
PH-08-02	1/24/08		31.0	8.18	12	577	2966	15	0	0.9	2235	145	1075	2033	1006	2515	a	685
PH-08-03[d]	1/24/08		30.6	7.87	11	136,752	7126	215	n.d.	0.0	98,199	3276	14,062	2457	555	−16,717	b	7390

(*continued on next page*)

Table 2 (*continued*)

Sample ID	Date	Discharge at sampling (m^3/sec)	*T* (°C)	pH	F (μmol/L)	Cl (μmol/L)	SO_4 (μmol/L)	Br (μmol/L)	NO_3 (μmol/L)	PO_4 (μmol/L)	Na (μmol/L)	K (μmol/L)	Mg (μmol/L)	Ca (μmol/L)	Si (μmol/L)	Alk (μeq/L)	Alk type[a]	TDS[b] (ppm)
PH-08-04	1/24/08		28.7	7.68	n.d.	2318	158	4	5	0.0	911	36	804	222	465	355	b	198
PH-08-05	1/25/08	3.7	23.3	8.10	0	36	28	n.d.	3	0.0	61	0	708	100	415	1612	a	150
PH-08-06	1/25/08	0.4	23.6	8.13	n.d.	41	33	n.d.	2	0.0	51	0	850	44	421	1790	a	163
PH-08-07	1/25/08	0.1	24.9	8.03	0	38	32	n.d.	n.d.	0.0	55	0	1291	53	729	2814	a	255
PH-08-08[d]	1/25/08		32.1	7.76	4	20,185	1092	29	n.d.	0.0	13,874	482	2885	648	625	-982	b	1234
PH-08-09	1/26/08	0.7	25.3	7.97	13	701	264	n.d.	210	15.1	1267	190	454	671	1672	2209	b	375
PH-08-10	1/26/08		26.8	7.96	15	330	152	n.d.	189	26.0	1236	281	551	770	1324	3338	a	408
PH-08-11	1/26/08	2.5	26.1	7.98	13	149	113	n.d.	81	9.9	703	159	401	639	1597	2733	a	343
PH-08-12	1/26/08		27.5	7.79	14	156	140	n.d.	54	5.8	678	153	406	690	1577	2779	a	347
PH-08-13	1/26/08	0.3	28.5	6.77	17	154	202	n.d.	245	9.4	632	178	426	641	1906	2371	a	358
PH-08-14	1/26/08		30.1	6.75	17	212	228	n.d.	n.d.	n.d.	805	232	511	823	1818	3267	a	411
PH-08-15	1/27/08	0.0	26.1	7.00	25	265	493	n.d.	354	6.2	989	264	643	1067	1646	3325	a	473
PH-08-17	1/27/08	0.3	26.9	7.13	20	280	227	n.d.	137	4.3	929	209	562	812	1727	3124	a	411
PH-08-18[d]	1/27/08		27.1	8.33	30	11,122	1089	13	n.d.	6.9	9989	850	1370	1044	34	2300	b	982
PH-08-19[d]	1/30/08		28.9	7.44	n.d.	26,234	1449	43	n.d.	0.0	19,104	787	2932	709	549	850	a	1727
PH-08-20	1/30/08		29.0	7.47	4	190	37	7	0	n.d.	318	56	172	406	913	1401	a	181
PH-08-21	1/31/08	0.4	29.3	7.45	18	222	238	n.d.	45	n.d.	629	127	343	498	1315	1676	b	263
PH-08-23	1/31/08	0.4	26.1	6.59	5	321	278	n.d.	0	0.0	592	84	340	627	1559	1949	a	301
PH-08-24	1/31/08	0.7	29.3	6.77	4	187	53	6	0	n.d.	354	77	169	236	1434	939	b	180
PH-08-25	1/31/08	1.2	28.6	6.46	3	182	112	n.d.	n.d.	n.d.	407	71	162	247	1272	885	b	174
PH-08-27	2/1/08		25.9	7.25	8	499	494	n.d.	7	0.0	609	98	539	558	1299	1398	b	282
PH-08-28	2/1/08	0.5	25.9	7.02	n.d.	142	64	n.d.	0	n.d.	359	50	134	195	1015	856	a	146
PH-08-29	2/1/08	0.9	26.0	6.56	4	234	211	n.d.	0	n.d.	300	40	138	200	731	357	b	114
PH-08-30	2/1/08		26.0	6.56	n.d.	1207	79	n.d.	n.d.	1.0	941	58	245	206	803	535	b	169
PH-08-32	2/1/08		25.8	7.60	n.d.	173	25	n.d.	n.d.	1.6	292	38	168	252	902	941	b	143
PH-08-33	2/1/08	0.0	24.3	7.16	17	183	85	n.d.	12	1.5	282	52	64	178	923	432	b	115
PH-08-34	2/1/08	3.2	26.3	7.85	n.d.	148	47	n.d.	n.d.	0.8	319	64	146	189	1231	810	b	154
PH-08-35	2/2/08	0.2	25.7	7.96	n.d.	144	35	n.d.	0	1.4	307	41	130	307	1184	1002	b	165
PH-08-36	2/2/08	0.2	24.9	8.11	n.d.	137	26	n.d.	0	n.d.	281	39	108	282	1161	908	b	154
PH-08-37	2/2/08	0.4	28.0	7.67	n.d.	184	78	n.d.	n.d.	0.0	344	49	233	423	1003	1365	b	190
PH-08-38	2/2/08		29.7	7.75	17	365	369	n.d.	48	3.0	665	105	586	1156	1174	3461	a	414
PH-08-39	2/2/08	0.8	29.3	8.15	n.d.	140	238	n.d.	0	0.0	432	31	1155	1235	667	4717	a	444
PH-08-40	2/3/08	1.3	24.8	8.12	13	117	58	n.d.	0	2.0	363	84	193	306	1250	1191	b	186
PH-08-41	2/3/08	12.4	24.8	8.06	n.d.	92	47	n.d.	8	n.d.	273	65	157	251	1162	959	b	159

PH-08-42	2/3/08	3.3	27.4	7.23	n.d.	199	162	n.d.	6	n.d.	282	64	128	221	921	513	b	131
PH-08-43	2/3/08	0.6	27.7	7.40	5	211	346	n.d.	0	0.7	280	56	122	288	800	245	b	127
PH-08-44	2/3/08	2.4	26.3	8.11	n.d.	100	76	n.d.	2	0.7	197	44	117	197	789	612	b	113
PH-08-45	2/3/08	2.2	26.0	6.85	n.d.	193	759	58	n.d.	0.0	452	62	216	363	1074	123	a	189
PH-08-46	2/4/08	1.4	25.7	7.52	n.d.	136	25	n.d.	n.d.	n.d.	176	28	93	117	466	438	b	74
PH-08-47	2/4/08	8.9	26.2	7.64	n.d.	130	26	4	n.d.	n.d.	202	37	100	153	728	559	b	100
PH-08-48	2/4/08		28.0	7.05	n.d.	187	23	n.d.	9	n.d.	257	54	96	179	826	619	b	114
PH-08-49	2/4/08		27.9	7.53	n.d.	128	38	n.d.	n.d.	n.d.	259	47	123	199	894	835	a	132
PH-08-50	2/7/08	0.2	23.9	8.33	7	61	141	n.d.	n.d.	n.d.	451	10	436	763	811	2508	b	270
PH-08-51	2/7/08	0.2	27.1	8.12	6	83	105	n.d.	27	5.3	229	40	271	1552	515	3954	a	363
PH-08-52	2/7/08	0.8	27.1	7.45	7	307	76	n.d.	78	n.d.	471	52	305	469	803	1528	b	204
PH-08-54	2/7/08	0.9	25.7	8.09	3	128	25	n.d.	n.d.	n.d.	252	60	167	213	788	981	a	135
PH-08-55	2/7/08	8.1	26.4	8.60	5	302	42	n.d.	24	2.7	344	87	293	258	1085	1106	b	178
PH-08-56	2/7/08		26.3	8.23	9	373	64	n.d.	75	5.6	434	108	389	331	1320	1379	b	225
PH-08-57	2/8/08	1.2	23.6	7.86	n.d.	141	35	n.d.	0	0.0	243	9	241	431	722	1385	b	165
PH-08-58	2/8/08		24.0	7.72	3	92	56	n.d.	0	0.0	203	11	197	657	533	1716	b	182
PH-08-59	2/8/08	5.7	24.2	8.22	3	131	39	n.d.	0	0.0	233	9	259	442	765	1430	b	171
PH-08-60	2/8/08	0.3	24.0	8.32	3	267	56	n.d.	0	0.0	270	16	179	480	819	1220	b	169
PH-08-61	2/9/08	2.2	27.7	8.61	3	91	81	n.d.	0	0.0	222	7	933	488	612	3009	a	279
PH-08-62	2/9/08	3.6	29.7	8.40	12	71	128	n.d.	27	0.0	308	13	696	486	712	2594	a	262
PH-08-63	2/9/08	1.7	30.7	8.17	14	4926	3286	n.d.	6	4.5	1720	181	884	2549	1097	2073	b	854
PH-08-64	2/9/08	0.4	28.2	8.18	n.d.	117	526	n.d.	0	4.0	581	95	431	845	1129	2047	b	309
PH-08-65	2/9/08	0.9	28.8	7.96	n.d.	756	798	n.d.	n.d.	5.0	1115	99	538	1233	1339	2837	a	450
PH-08-66	2/10/08	0.3	28.0	8.24	21	766	4712	n.d.	n.d.	3.2	2447	235	848	3621	1369	1830	a	906
PH-08-67	2/10/08	0.5	29.3	7.99	15	1832	4486	n.d.	0	n.d.	3249	291	1107	3220	1237	1691	a	916
PH-08-68	2/10/08	1.1	29.6	7.95	n.d.	775	2820	n.d.	71	n.d.	1675	203	990	1927	1481	1398	a	625
PH-08-70	2/10/08	0.0	33.7	7.41	n.d.	244	336	n.d.	113	2.2	666	167	295	481	1297	1349	b	257
PH-08-71	2/10/08	2.0	29.0	8.29	n.d.	1321	612	n.d.	0	n.d.	1389	94	440	894	876	2005	a	363
PH-08-72	2/10/08	0.2	30.0	7.63	n.d.	66	143	n.d.	n.d.	1.7	414	77	265	455	1158	1574	b	219
PH-08-73	2/10/08	1.9	31.2	7.47	n.d.	579	1963	n.d.	35	2.5	1304	192	765	1495	1437	1810	a	524
PH-08-74	2/10/08	0.3	29.6	8.22	n.d.	1239	1109	n.d.	n.d.	3.0	1556	146	719	1507	913	3027	a	510
M178	n.a.	n.a.	n.a.	–	14	1768	1938	0	27	6	36	6	19	51	242	5463	b	603

[a] a = determined by Gran titration, b = determined by charge balance.

[b] TDS = $Na + K + Ca + Mg + F + Cl + SO_4 + Br + NO_3 + PO_4 + HCO_3 + SiO_2$.

[c] Hot spring.

[d] Sample not included in flux analysis due to possible seawater contamination.

[e] n.d. = not detected.

Table 3
Sr concentration and isotopes of Luzon rivers, 2007 and 2008.

Sample ID	Sr (nmol/L)	$^{87}Sr/^{86}Sr$	± (2σ)
PH-07-01	438	0.70441	0.00012
PH-07-02	436	0.70335	0.00008
PH-07-03	808	0.70469	0.00010
PH-07-05	911	0.70802	0.00008
PH-07-06	3760	0.70421	0.00012
PH-07-07	2093	0.70438	0.00010
PH-07-08	892	0.70446	0.00008
PH-07-09	1278	0.70449	0.00010
PH-07-12[a]	6760	0.70364	0.00008
PH-07-13	4053	0.70359	0.00007
PH-07-15	2742	0.70394	0.00007
PH-07-16	1221	0.70379	0.00007
PH-07-19	1337	0.70380	0.00007
PH-07-20	2031	0.70402	0.00008
PH-07-22[a]	3895	0.70396	0.00007
PH-07-25	1953	0.70639	0.00010
PH-07-26	927	0.70384	0.00008
PH-07-28	872	0.70432	0.00007
PH-07-29	914	0.70394	0.00008
PH-07-30	1452	0.70382	0.00007
PH-07-31	1186	0.70465	0.00007
PH-07-32	1058	0.70479	0.00008
PH-07-33	137	0.70383	0.00012
PH-07-34	600	0.70433	0.00008
PH-07-35	423	0.70394	0.00008
PH-07-36	467	0.70381	0.00012
PH-07-37	469	0.70433	0.00008
PH-07-39	464	0.70383	0.00012
PH-07-40	462	0.70377	0.00012
PH-07-41	691	0.70430	0.00008
PH-07-42	637	0.70438	0.00007
PH-07-43	552	0.70480	0.00008
PH-07-44	350	0.70418	0.00007
PH-08-01	747	0.70451	0.00010
PH-08-03[b]	19732	0.70904	0.00010
PH-08-06	61	0.70488	0.00012
PH-08-07	72	0.70527	0.00012
PH-08-08[b]	3586	0.70890	0.00015
PH-08-09	1162	0.70491	0.00007
PH-08-10	1706	0.70494	0.00007
PH-08-11	1192	0.70467	0.00038
PH-08-12	1319	0.70512	0.00015
PH-08-13	1019	0.70520	0.00007
PH-08-15	1413	0.70485	0.00007
PH-08-17	1135	0.70504	0.00007
PH-08-18[b]	1614	0.70552	0.00022
PH-08-21	1504	0.70382	0.00010
PH-08-23	1459	0.70399	0.00009
PH-08-24	947	0.70414	0.00015
PH-08-27	1482	0.70412	0.00008
PH-08-28	903	0.70439	0.00010
PH-08-30	1157	0.70481	0.00008
PH-08-41	1112	0.70380	0.00008
PH-08-45	1383	0.70359	0.00013
PH-08-54	836	0.70435	0.00007
PH-08-58	769	0.70593	0.00008
PH-08-68	5782	0.70421	0.00008
M178	389	–	–

[a] Hot spring.
[b] Possible seawater contamination.

is based on the finished-grade 3 arc-second NASA SRTM data. SRTM data suffer from data voids, especially over water bodies and in mountainous areas, and the CGIAR-CSI dataset has been processed to fill those data voids using auxiliary data (Reuter et al., 2007). The CGIAR DEM was processed in ArcGIS 9.3 and ArcINFO (ESRI, 2009). Sinks in the DEM were identified and filled with ArcGIS Spatial Analyst functions. Watersheds were created for all rivers and streams sampled, as well as for all rivers for which historical runoff data is available.

The runoff data used was collected by the National Water Resources Council (NWRC) of the Philippines and made accessible to us by Professor Glenn Tabios at the Department of Hydraulics at the University of the Philippines, Diliman. The NRWC divides the Philippines into 10 water resources regions (WR); the ones we worked in are WR 3 (Central Luzon), WR 4 (Southern Tagalog) and WR 5 (Bicol). We used two data sets, one from 1944 to 1970 and another from 1982 to 2000 (only a few streams were monitored for the entire period). The average duration of data collection for the streams we used was 10 years for streams draining ophiolites and 12 years for streams draining volcanic areas, with minimum of 6 and 2 years and maximum of 14 and 24 years, respectively. The data do not contain any estimates of uncertainty for individual discharge measurements. Most of the rivers and streams have approximately normally distributed yearly discharge, allowing us to use arithmetic average and standard deviation to assess uncertainty in the dataset.

Simple *t*-tests, performed using the JMP 8.0 software package (SAS, 2009), reveal no significant differences between average runoff by geographic region or lithology. The variation in runoff (coefficient of variation (CV, %) = standard deviation/mean × 100%) in ophiolitic regions is significantly less (CV = 25%), than in volcanic regions (CV = 47%). We cannot tell if the difference in CV between lithologies is caused by variations in data availability and duration of records or if it is caused by variability in climate in the different regions. The spatial distribution of the mean runoff was investigated using ArcGIS 9.3 software (ESRI, 2009). No spatial trends in average runoff were detected, rendering spatial interpolation methods such as Kriging or nearest neighbor interpolation inappropriate for predicting runoff in unmonitored basins.

Multiple linear regression was performed on the calculated average runoff for each basin using JMP 8.0. The predictors we used were landscape metrics that are readily available for each basin, namely the average, minimum, maximum and standard deviation of each of the following; elevation, slope and aspect. Any of these variables individually have very little predictive potential for mean runoff ($r^2 = 0$–0.4). Multiple linear regression models of average runoff yielded better r^2 for several combinations of independent variables (r^2 of modeled vs. observed runoff >0.98), but cross-correlation between variables and unrealistic model parameters indicate that the good fit is artificial. In short, the results of statistical treatment of the runoff data indicate that none of the potential predictor variables we tested have any real predictive potential.

We therefore use the regionally averaged observed runoff to calculate discharge in unmonitored watersheds. We distinguish between watersheds in ophiolitic and volcanic regions, using the average runoff (2539 mm/yr and 2106 mm/yr, respectively) for unmonitored streams. Several of the streams we studied drain a mix of ophiolitic and volcanic bedrock. For these streams, we use the statistics for rivers draining volcanic regions.

3.4. Uncertainty propagation in flux calculations

Uncertainty in chemical analyses, watershed area and stream discharge were propagated through flux calculations according to the methods presented in Bevington and Robinson (2002).

Chemical fluxes of a given element, X, from a watershed, i, are calculated as the concentration of that element, $[X]$, multiplied by the discharge, Q, through the watershed, Q_i: $[X] \times Q_i$. Q_i is the product of runoff through the watershed and the area of the watershed, A_i. Uncertainties in the area of watersheds are taken from Oksanen and Sarjakoski (2005). Their study utilized DEMs with a cell size of 10 m, and we apply their results unchanged to the 90 m-resolution DEM used in our study. According to Oksanen and Sarjakoski (2005), CV is 24% in watersheds smaller than 2 km^2, 16% in watersheds between 2 and 22 km^2 and less than 3% in watersheds larger than 22 km^2.

The CV for total (t) chemical fluxes (F) in a single watershed i, (Ft, i), is calculated as:

$$\mathrm{CV}_{Ft,i} = \sqrt{\mathrm{CV}_{[X]}^2 + \mathrm{CV}_{Q_i}^2} \tag{2}$$

In the case of area-normalized (a) fluxes (F) through a single watershed i, (Fa, i), the equation becomes:

$$\mathrm{CV}_{Fa,i} = \sqrt{\mathrm{CV}_{Ft,i}^2 + \mathrm{CV}_{A_i}^2} \tag{3}$$

Watersheds are aggregated into regions. The CV for the total chemical fluxes from a region j, (Ft, j), is calculated as:

$$\mathrm{CV}_{Ft,j} = \sqrt{\frac{\sum_{n=1}^{i}\left[\mathrm{CV}_{Ft,i}^2 \times Q_i\right]}{\sum_{n=1}^{i} Q_i}} \tag{4}$$

In the case of area-normalized fluxes from a region j, (Fa, j), the equation becomes:

$$\mathrm{CV}_{Fa,j} = \sqrt{\frac{\sum_{n=1}^{i}\left[\mathrm{CV}_{Fa,i}^2 \times A_i\right]}{\sum_{n=1}^{i} A_i}} \tag{5}$$

4. RESULTS AND DISCUSSION

4.1. Major elements

In Table 2, chemical analyses of our samples are listed. We divide the rivers studied into two very broad classes, ophiolites and volcanic regions. Within each class the major element chemistry of the streams (Na^+, K^+, Ca^{2+}, Mg^{2+}, Cl^-, SO_4^{2-} and HCO_3^-) is broadly similar, but there are pronounced differences between the two classes. Rivers draining ophiolites have significantly (at 95% significance level) higher pH values and a smaller range in pH than volcanic rivers (average pH of 8.2 and 7.6, respectively). The higher pH in ophiolite waters may be caused by low-temperature serpentinization (Neal and Shand, 2002). The large range in the pH of volcanic rivers is a result of some, but not all, of those rivers receiving addition of magmatic gases and acids.

Bicarbonate is the dominant anion in most of the rivers sampled (Fig. 4). Cl^- contributes the major negative charge to only two rivers, Salaza River in Zambales (PH-08-04) and Bangon River in Sorsogon (PH-08-30). Neither of the two rivers shows other obvious signs of seawater input (such as high $^{87}Sr/^{86}Sr$). Sulfate is a major contributor to the negative charge in rivers draining Mount Pinatubo and in a few rivers draining volcanic craters on the Bicol Peninsula.

Mg^{2+} is a major contributor to the positive charge in ophiolitic rivers, especially in the Zambales ophiolite, and most of these rivers contain insignificant amounts of Na^+ and K^+. The cation component of volcanic rivers has roughly subequal contributions from the major components; in most cases $Ca^{2+} > Mg^{2+} > (Na^+ + K^+)$. No systematic difference in either anion or cation composition exists between rivers draining the BVA vs. the LVA, indi-

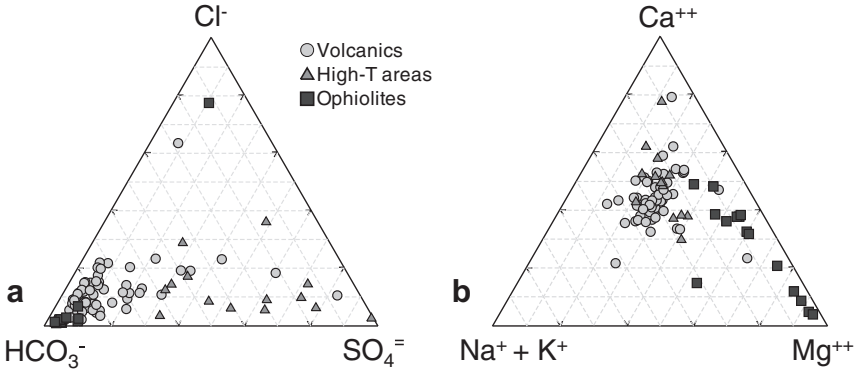

Fig. 4. Ternary diagrams of the major anion and cation composition of the rivers studied. The diagrams show the river water composition in terms of charge equivalents and are not corrected for atmospheric or hydrothermal inputs. Bicarbonate is the dominant anion in systems other than those with active volcanic activity. Ophiolite streams are, as expected, Mg-rich.

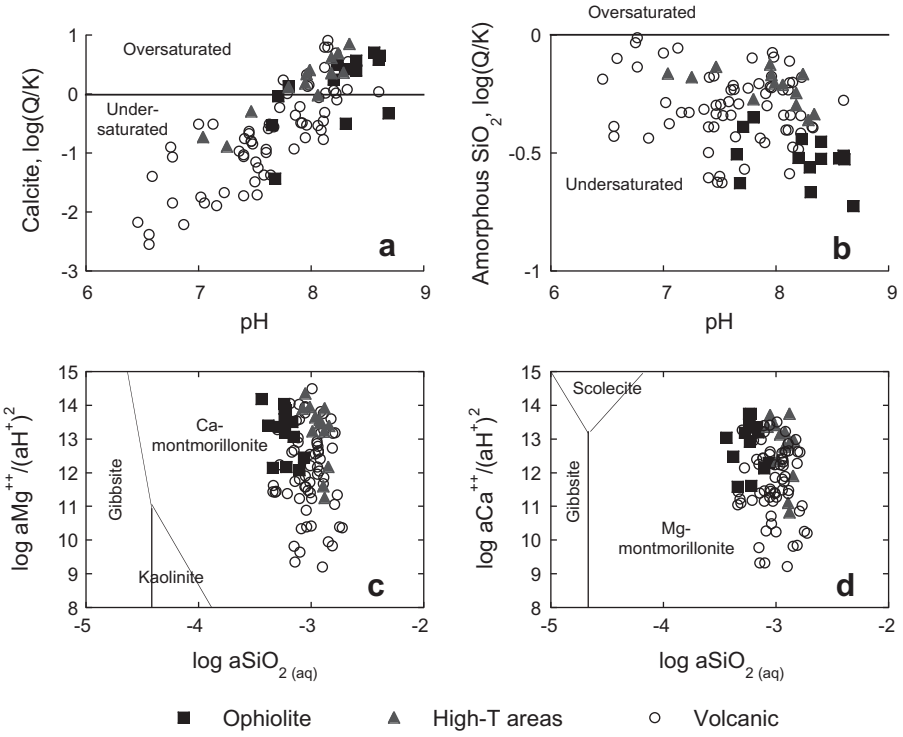

Fig. 5. Mineral saturation diagrams for the rivers under study. Calculated using Geochemist's Workbench 7 at $T = 25$ °C. Saturation index as a function of pH for (a) calcite and (b) amorphous silica. Stability diagrams for (c) Mg and (d) Ca indicate that the river water is in the stability field of secondary smectite minerals.

cating similar weathering conditions and processes in these two regions.

We calculated the saturation state of the waters studied with respect to primary and secondary minerals using Geochemist's Workbench 7.0 (Bethke, 2007). Calcite saturation is prevalent in waters at pH > 8, regardless of whether the lithology is volcanic or ophiolitic (Fig. 5a). In general, rivers draining ultramafic rocks have higher pH and are more likely to be supersaturated with calcite. Rivers draining the BVA are usually undersaturated with calcite, even at pH over 8, while rivers draining the LVA are more likely to be saturated with calcite. The streams we studied generally have high concentrations of dissolved Si: 412–885 μM in ophiolites, 466–1906 μM in volcanics. These values are similar to or higher than those reported from basaltic islands: 270–1250 μM in Sao Miguel rivers (Louvat and Allegre, 1998), 420–2700 μM in Iceland rivers (Gislason et al., 1996) and 280–570 μM in Reunion rivers (Louvat and Allegre, 1997). Many of our samples are close to opal saturation (Fig. 5b) but we have not attempted to determine the influence of plant uptake on silica fluxes (Derry et al., 2005).

Total dissolved solids (TDS) in streams in Luzon (150–332 and 82–916 mg/L in ophiolite and volcanic streams, respectively) are high compared to world rivers (50 mg/L in the Amazon) (Meybeck and Ragu, 1995) and similar to or higher than TDS observed in other volcanic regions mentioned above. Luzon streams tend to have high cation concentrations compared to other volcanic provinces such as the Stikine terrane (Gaillardet et al., 2003), the Azores (Louvat and Allegre, 1998), New Zealand (Goldsmith et al., 2008) and Iceland (Gislason et al., 1996). This is especially true for Mg^{2+} and Ca^{2+}, even when excluding ophiolite streams. The high cation concentrations coupled with the high Si concentration put the water into the stability fields of smectites (Fig. 5c and d); smectites are the most common clay mineral in river sediments on Luzon (smectites on average comprise 86% of clay abundances, Liu et al. (2009)). These observations are consistent with expectations of fast weathering of ultramafic to intermediate compositions with fine-grained to glassy textures, in a volcanically and tectonically active area with a warm and humid climate.

4.2. Sr isotopes

Measured Sr concentrations in the rivers and streams sampled here are 61–911 nmol/L for ophiolites and 426–9884 nmol/L for volcanics. The highest values are generally found in the Pinatubo area and are likely caused by high-temperature weathering (hydrothermal) activity, low flow at time of sampling or a combination of those two factors. The only other study to report dissolved river data from the Philippines, as far as the authors are aware, is that of Goldstein and Jacobsen (1987) where values of 102–172 ppb Sr (1164–1963 nmol/L) were reported for four rivers draining central and northern Luzon. The $^{87}Sr/^{86}Sr$ values for dissolved riverine Sr reported by Goldstein and Jacobsen (1987) are somewhat higher than those reported here, ranging from 0.70452 to 0.70628. None of those four rivers drains exclusively volcanic lithologies and the

presence of Sr derived from sedimentary sources likely explains the higher values.

The Sr isotope signature of river water reflects the relative contribution of atmospheric inputs and chemical weathering of the various lithologies that make up the watershed to the solute load. We consider three end members; rainwater, limestones and igneous rocks. We take the value of Sr in precipitation to be that of modern seawater, 0.7092. Marine limestones in the Philippines are mostly Miocene and younger and we adopt an average value of 0.7088 for limestone in this work (McArthur et al., 2001). The Sr isotope signature of volcanic rocks in the study area is given in Table EA2. For regions without published $^{87}Sr/^{86}Sr$ data we use the overall mean of the data from volcanic regions, $^{87}Sr/^{86}Sr = 0.70400 \pm 0.00066$ (Knittel-Weber and Knittel, 1990; Castillo and Newhall, 2004; McDermott et al., 2005; DuFrane et al., 2006). We measured Sr isotopes on 53 of the water samples presented here. A large majority of these samples (45 of 53 samples, or 85%) has $^{87}Sr/^{86}Sr$ ranging between 0.7036 and 0.7050, showing little evidence of dissolution of marine carbonate or any large contribution of rainwater.

Eight samples, or 15% of measured samples, have $^{87}Sr/^{86}Sr$ higher than 0.7050. These samples were assumed to reflect a mix of Sr from igneous rocks and limestone (where geological map revealed presence of marine carbonate within the basin) or igneous rocks and rain (where, according to geological maps, no marine carbonate is present in the basin). We used a simple two-component mixing model to partition the Sr in those high-$^{87}Sr/^{86}Sr$ samples into relative proportions derived from igneous rock and limestone/rain:

$$f_i = \frac{R_{spl} - R_a}{R_i - R_a} \times 100 \quad (6)$$

where "f" refers to fractional contribution, "R" refers to $^{87}Sr/^{86}Sr$ and the subscripts "i" and "spl" refer to igneous rock and sample, respectively. The subscript "a" refers to limestone or rain, as the case may be.

Of the watersheds we studied ($n = 75$), available geological maps indicate that only three basins have appreciable amounts of marine carbonates. Sr-isotope analyses were made on all of those rivers; the Masinloc River on the west coast of the Zambales ophiolite, the Sipocot River which drains Mt. Labo and the surrounding lowlands in the provinces of Camarines Norte and Sur, and the Agus River in the Southern Sierra Madre Mountains. The contribution of weathering of limestone to the dissolved Sr load of these rivers is 82%, 52% and 25%, respectively. Of the remaining 72 watersheds, only 4 have significantly elevated $^{87}Sr/^{86}Sr$. Three of those drain Taal Volcano in Batangas Province, (Palico, Obispo and Dacanlao streams). Geological maps do not show any carbonate outrcops in these watersheds but the Sr isotope data and the spatial arrangement of the affected watersheds, which all lie adjacent to each other, indicate the likely presence of a subsurface body of carbonate rocks. The proportion of limestone-derived Sr in those streams ranges from 11% to 15%. The fourth stream is an ephemeral tributary of the Lawis River in the Zambales ophiolite, which has about 16% rain-derived Sr.

Table 4
Cl-normalized molar ratios used in solute partitioning calculations.

	SO_4/Cl	Na/Cl	Ca/Cl	K/Cl	Mg/Cl	HCO_3/Cl
Rainfall[a]	0.052	0.858	0.019	0.019	0.098	–
Hydrothermal fluids[b]	1.065	0.636	0.535	0.181	0.326	1.122

[a] Sea salt ratios from Schlesinger (1997).
[b] Average of published data (see text for references) and samples PH-07-12 and PH-07-22.

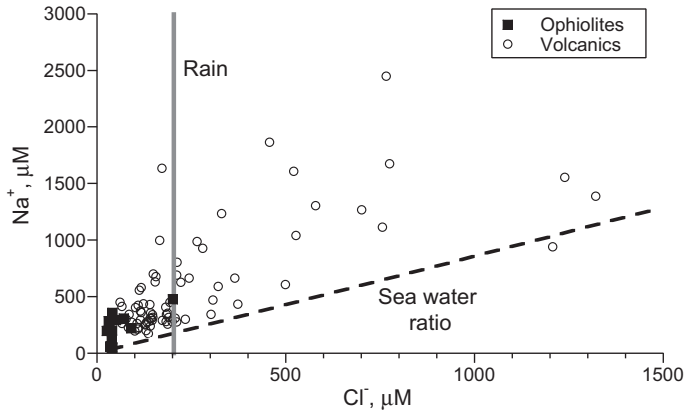

Fig. 6. Significant enrichment of Na^+ in river water from what would be expected if all Na^+ originated in rainfall with Na/Cl of 0.86. The excess Na^+ is derived from weathering. The estimate of 200 µM Cl^- in rain is derived form regional average rainfall values (100 µM) and an evapotranspiration factor of 2.

4.3. Sources of solutes

In volcanic areas, stream chemistry is influenced not only by low-temperature (low-T) weathering and atmospheric deposition but also by geothermal processes, which we refer to as high-temperature (high-T) weathering. The mass-balance equation for a conservative element X is:

$$[X]_{tot,i} = [X]_{rain,i} + [X]_{\text{high-T},i} + [X]_{\text{low-T},i} \quad (7)$$

where $X = \{Na^+, K^+, Ca^{2+}, Mg^{2+}, SO_4{}^{2-}\}$, the subscript "$i$" refers to each individual stream, "*tot*" refers to the total concentration of X, and "*rain*" refers to solutes derived from atmospheric inputs.

We calculate the contributions from atmospheric and geothermal inputs from end member models and assume that low-T weathering makes up the rest. To correct for the atmospheric deposition of the major elements, we use sea salt X/Cl ratios, listed in Table 4, and $[Cl]_{rain,i}$ for all streams, such that:

$$[X]_{rain,i} = \left(\frac{X}{Cl}\right)_{\text{sea salt}} \times [Cl]_{rain,i} \quad (8a)$$

Combined high- and low-temperature weathering products are referred to as X^*:

$$[X]^* = [X]_{tot,i} - [X]_{rain,i} \quad (8b)$$

A significant contribution of Na^+ from weathering is evident in a plot of Na^+ vs. Cl^-, showing $(Na^+/Cl^-)_{\text{stream}} > (Na^+/Cl^-)_{\text{sea salt}}$ (Fig. 6). We assume that the maximum plausible Cl^- concentration in volcanic streams unaffected by hydrothermal activity is 200 μM. If $[Cl^-]_{tot,i} < 200$ μM, all Cl^- is assumed to come from atmospheric deposition. The value of $[Cl^-]_{rain} = 200$ μM derives from the assumption that rainfall in the region has an average chloride concentration of 100 μM (Eklund et al., 1997; Waterloo et al., 1997; Fujita et al., 2000; Kyoung Lee et al., 2000) and the evapotranspiration factor is around 2. Inputs from Cl^- bearing minerals such as amphiboles are believed to be minor and in any case are not well constrained by our data. All Cl^- in streams draining ultramafic areas is attributed to atmospheric input since no hydrothermal activity is reported in these areas.

Next, we correct for hydrothermal (high-T) contribution to streams draining volcanic regions. We adopt the method used by Dessert et al. (2009) to calculate the contribution of high-temperature weathering to the dissolved load:

$$[Cl]_{\text{high-T},i} = [Cl]_{tot,i} - [Cl]_{rain,i} \quad (9a)$$

and

$$[X]_{\text{high-T},i} = \left(\frac{X}{Cl}\right)_{\text{hot springs}} \times [Cl]_{\text{high-T},i} \quad (9b)$$

The only exception from this order of corrections is $HCO_3{}^-$. First we correct for hydrothermal input using the HCO_3/Cl ratio of hydrothermal waters and then we attribute the remaining HCO_3 to atmospheric origin.

For the hot spring end member X/Cl we use the average of our own data from hot springs sampled on Mt. Isarog and Mt. Bulusan and published data from three Philippine hydrothermal areas; Pinatubo (Stimac et al., 2004), Taal (Delmelle et al., 1998) and Manito-Bacon (Baltasar, 1980), see Table 4. Model runs where we used the regional average of $(X/Cl)_{\text{hot springs}}$ did not yield significantly different results than using the average of all available data. Given that result and the fact that the range in composition of hydrothermal fluids is quite large, we prefer to use all the data available to us to constrain the end-member ratios for the hot springs.

We carried out a sensitivity analysis to investigate the impact of varying the end member assumptions on the solute source allocations (Appendix 1), investigating 27 different scenarios. The sensitivity analysis was carried out independently of the flux calculations and their associated uncertainties (Section 3.4), and deals with the possible variability in the fractional contribution of the three sources (rain, hydrothermal end member, low-temperature weathering end member) to the total chemical flux.

In volcanic areas, variability in the composition of rainfall causes variability in the fraction of solutes derived from rainfall of 11% (Mg) to 67% (Ca). The observed variability in the composition of hydrothermal fluids leads to variability in the fraction of solutes derived from these fluids of 16% (the alkali metals) to 22% (Mg). These values may seem high, but it should be kept in mind that both rainfall and high-T weathering are relatively small components of the overall solute flux. A confirmation of this effect is evident in the modeled variability in the fraction of solutes from low-T weathering; it is small, ranging from 2.4% (the alkaline earths) to 9.6% (K^+). In ophiolite regions the variability in source allocation is much smaller; it is always less than 1% in the case of precipitation and in the case of low-T weathering solutions, it ranges from >1% (the alkaline earths) to 35% (K^+). We therefore conclude that our estimates of absolute solute fluxes from the three different sources are relatively insensitive to the exact ratios used in solute partitioning calculations.

The Philippines is a densely populated country (89 million) with nearly 300 inhabitants/km^2. Agriculture is a major land use in the Philippines, covering some 32% of the islands (http://countrystat.bas.gov.ph). Significant soil erosion and modification of the natural ecosystem by humans has occurred in the Philippines over the 20th century (see e.g., Kastner, 2009). Furthermore, many of the streams sampled run through urban areas where untreated wastewater is channeled directly into streams and lakes (Dyer et al., 2003). These conditions can influence the dissolved load chemistry of streams, although their impact on silicate weathering budgets is less clear. Unfortunately, we are not aware of any studies that can be used to quantify the impact of human land use in the Philippines on weathering chemistry. For the present, we simply note that land use is an additional source of uncertainty in our weathering flux calculations but one that is not currently constrained.

4.3.1. Regional trends in sources of solutes – atmospheric inputs

No spatial trends were observed in the exports of rain-derived solutes. In terms of species concentrations in individual samples, Cl^- from rainfall ranges from nearly 0% in the Pinatubo region (O'Donnell River) to 100% in the

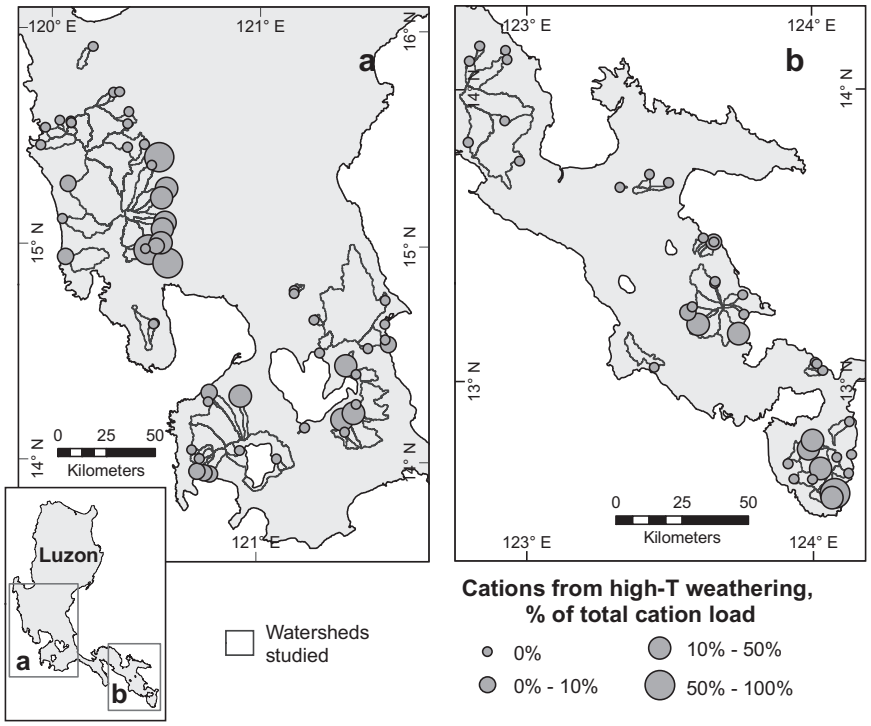

Fig. 7. Percent of total cation load derived from high-temperature weathering, calculated using Cl as indicator for high-T weathering (Dessert et al., 2009). The method correctly identifies numerous streams draining active volcanoes as heavily impacted by high-T weathering activity but fails to identify one stream that is heavily impacted by inputs of magmatic sulfuric acid.

majority of volcanic streams and ophiolite streams. The regional average $\%Na_{rain}$ ranges from 13% (Pinatubo) to 46% (Quezon) and average $\%K_{rain}$ is 2–6% in volcanic areas and ~27% in the ophiolites and in Quezon. Rain-derived Ca^{2+} never exceeds 2% of the total Ca^{2+} concentration in any region studied and the $\%Mg_{rain}$ is only slightly higher than $\%Ca_{rain}$ in most regions.

4.3.2. Regional trends in sources of solutes – high-temperature weathering

We assessed the validity of the method of Dessert et al. (2009) by plotting the cation load derived from high-temperature processes as a percentage of the total cation load due to silicate weathering on a map of Luzon (Fig. 7). As described above, this method relies on Cl^- as indicator element for hydrothermal activity and this may limit its usefulness in hydrothermal systems dominated by other acids than HCl. Overall, the method yields plausible results although it fails to replicate large observed inputs of hydrothermal fluids into Rangas River on the Bicol Peninsula, which drains the crater of Isarog volcano. This system appears to be dominated by sulfuric acid, judging by the large proportion of sulfate in the water and strong smell of sulfur at the river.

The highest percentages of hydrothermal inputs cluster around major volcanoes (Pinatubo, Mayon, Bulusan), just as expected from field observations and published data. The exception is rivers on the flanks of Taal Volcano, where the Dessert method predicts only small amounts of high-temperature inputs, contrary to what might be expected from the presence of a very active hydrothermal system inside the Taal caldera (Delmelle et al., 1998). Most of the streams sampled on Taal drain the outside flanks of the caldera and we infer that the impact of the hydrothermal system extends only to a small extent to the outer flanks of the caldera. Hydrothermal inputs into the streams SE of Laguna de Bay most likely come from the numerous maars that dot the landscape in that area.

Hydrothermal activity supplies on average approximately 10% of the dissolved cation load in the volcanic rivers we studied. The range is very large; most streams are not affected by hydrothermal activity while others get most of their solutes from hydrothermal activity.

4.3.3. Regional trends in sources of solutes – low-temperature weathering

Area-normalized exports of cations produced by low-temperature weathering are largest in the Pinatubo area ($5.44 \pm 0.81 \times 10^6$ mol/km^2/yr) but smallest in the Camarines region ($1.26 \pm 0.22 \times 10^6$ mol/km^2/yr). Most valleys draining the Pinatubo complex are still filled with voluminous lahar deposits from the cataclysmic 1991 eruption (Montgomery et al., 1999) and the large surface area of these deposits no doubt contributes to the high weathering fluxes in the region. It is also quite possible that our method underestimates hydrothermal inputs somewhat and that the solute load is differently distributed between low- and high-temperature sources. The relatively small low-temperature cation exports from the Camarines region may be biased by the relatively high discharge, and thus low solute concentrations, of rivers when sampling took place.

If calcium and magnesium are investigated separately, area-normalized low-temperature fluxes from Pinatubo and

Table 5
Fluxes of silicate-weathering derived solutes and atmospheric carbon from Luzon, 2007 and 2008.

Region	Area sampled	Silicate weathering cation flux[a]			Silicate weathering Ca* + Mg* flux	Silicate weathering flux[b]	SO_4 flux	Silicate weathering carbon export flux[c]	Silicate weathering carbon sequestration flux[d]
	km^2	10^9 mol/yr	10^9 eq/yr	10^5 t/yr	10^9 mol/yr	10^5 t/yr	10^9 eq/yr	10^9 mol/yr	10^9 mol/yr
Total flux									
ZA[e]	930	3.13	5.87	0.90	2.74	1.77	0.06	5.57	2.94
Bicol	401	1.50	2.54	0.46	1.04	1.00	0.15	1.94	1.13
Camarines	736	0.93	1.56	0.29	0.63	0.85	0.02	1.72	0.92
Sorsogon	322	0.97	1.55	0.29	0.57	0.78	0.21	0.99	0.66
BLM[f]	696	1.33	2.25	0.42	0.92	1.22	0.07	2.02	1.03
Pinatubo[g]	1727	14.43	23.42	4.44	8.99	6.83	6.44	8.56	9.95
Quezon	1028	1.50	2.69	0.49	1.19	1.18	0.03	2.98	1.54
Taal	708	3.02	4.71	0.93	1.69	2.35	0.14	4.38	1.98
Volcanic, all	5618	23.69	38.71	7.32	15.02	14.21	7.06	22.59	17.22
	km^2	10^6 mol/km^2/yr	10^6 eq/km^2/yr	t/km^2/yr	10^6 mol/km^2/yr	t/km^2/yr	10^6 eq/km^2/yr	10^6 mol/km^2/yr	10^6 mol/km^2/yr
Area-normalized flux									
ZA	930	3.36	6.32	97	2.95	190	0.07	5.99	3.16
Bicol	401	3.75	6.33	115	2.59	249	0.36	4.84	2.83
Camarines	736	1.26	2.11	40	0.85	116	0.03	2.33	1.25
Sorsogon	322	3.02	4.80	90	1.78	243	0.66	3.07	2.06
BLM	696	1.91	3.23	61	1.32	175	0.10	2.90	1.48
Pinatubo	1727	8.36	13.56	257	5.20	396	3.73	4.96	5.76
Quezon	1028	1.46	2.61	48	1.16	114	0.02	2.90	1.50
Taal	708	4.27	6.66	131	2.39	332	0.19	6.19	2.80
Volcanic, all	5618	3.75	6.13	116	2.38	225	1.12	3.58	2.73

[a] Silicate weathering cation flux = Na* + K* + Ca* + Mg*.
[b] Silicate weathering flux = silicate cation weathering flux + SiO_2.
[c] Total bicarbonate flux, also called "carbon consumption" in published studies.
[d] See France-Lanord and Derry (1997, p. 66).
[e] ZA = Zambales and Angat ophiolites.
[f] BLM = Bataan, Laguna and Macolod.
[g] Pinatubo = comprises both streams draining exclusively Pinatubo and streams draining both Pinatubo and the adjacent Zambales ophiolite.

Camarines are still the largest and smallest, respectively. The Zambales and Angat ophiolites have the second largest fluxes of Ca and Mg, consistent with their ultramafic lithology.

Area-normalized exports of Si from the Bicol Peninsula show a weak but highly significant ($R^2 = 0.27$, $p_{slope} < 0.001$) correlation with age of the substrate, increasing from a regional average of $1.27 \pm 0.21 \times 10^6$ mol/km^2/yr in Camarines, the oldest part of the currently active BVA, through $2.23 \pm 0.31 \times 10^6$ mol/km^2/yr in Bicol to a regional average of $2.54 \pm 0.35 \times 10^6$ mol/km^2/yr in Sorsogon, the youngest part of the Bicol Peninsula. Two factors may contribute to this trend. The basins developed on younger substrates have more hydrothermal input, while weathering of the older substrates may have partially depleted Si as soils evolve, resulting in lower modern Si fluxes.

4.4. Element fluxes

A full understanding of the controls on weathering fluxes in tectonically or volcanically active regions includes disentangling the signatures of high- and low-temperature inputs (Evans et al., 2004; Dessert et al., 2009). We argue that once in the ocean, base cations derived from high-T weathering (i.e., released by the action of strong acids such as HCl and H_2SO_4) of silicate rocks have the same potential to form sedimentary carbonates and sequester carbon as solutes from low-temperature weathering, even if no carbon was consumed and exported during the release of these cations. This is because in the ocean, where solutes from a large number of weathering systems come together, these high-T cations can form carbonates with bicarbonate derived from silicate weathering of alkali metals in other weathering systems. In particular, sulfate reduction generates alkalinity that can then be removed by reaction with cations that were originally dissolved by sulfuric acid. Consequently, high-T weathering of silicate rocks has similar implications for the long term carbon cycle as silicate low-T weathering. In the following discussion, we therefore treat high- and low-temperature weathering products as a single category, solutes derived from silicate weathering (X^*).

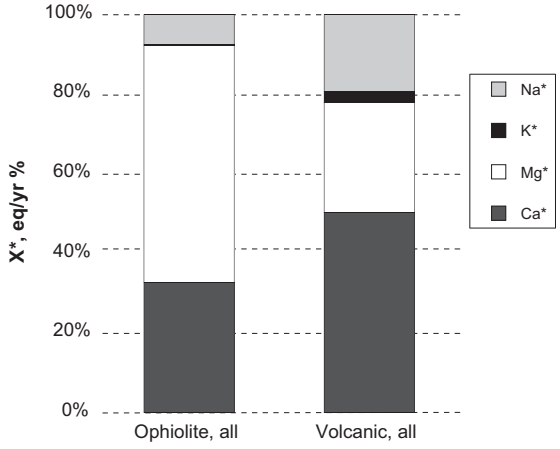

Fig. 8. Partitioning of elements (by charge) derived from weathering in rivers draining ophiolites and volcanic regions on Luzon. The dominance of Ca and Mg in both classes of rivers is apparent. Mg is the dominant cation in ophiolitic rivers and Ca in volcanic rivers. K is almost completely absent in the solute load of ophiolitic rivers, reflecting its scarcity in ultramafic rocks (and possible uptake by vegetation).

The area-normalized fluxes of major elements from the Philippine watersheds studied are among the highest recorded anywhere in the world (see Tables 5, EA3 and EA4). Export of cations derived from silicate weathering is 35–241 t/km^2/yr in volcanic areas and 54–147 t/km^2/yr in ophiolitic regions. Silicate weathering rates (cation weathering rate plus silica, calculated as SiO_2) are 108–380 t/km^2/yr in volcanic and 119–283 t/km^2/yr in ophiolitic regions, respectively. This compares to silicate weathering rates of 0.8 (Ob) to 72 t/km^2/yr (Irrawaddy) in some of the world's largest rivers (Gaillardet et al., 1999) and of 15–310 t/km^2/yr in volcanic regions of New Zealand (Goldsmith et al., 2008).

The volume-weighted average composition of waters draining ophiolitic and volcanic areas is shown in Fig. 8. The data has been corrected for precipitation inputs and limestone dissolution where necessary. Ophiolitic rivers are very Mg-rich compared to volcanic rivers (~60% vs. ~30% on equivalent basis, respectively) and the combined Mg and Ca contribution to the solute load in these rivers is over 95%. This explains the very high alkalinity of rivers draining ultramafic rocks. Ca and Mg are also the most important components of volcanic rivers, accounting for a little less than 80% of the cationic charge. Area-normalized fluxes of dissolved Ca and Mg from ultramafic areas ($2.95 \pm 0.25 \times 10^6$ mol/km^2/yr) are on the high end of the range observed in volcanic regions ($0.76–4.86 \times 10^6$ mol/km^2/yr), mainly due to the very large contribution of Mg to the dissolved load. Dissolved Si flux in ophiolite rivers ($1.55 \pm 0.13 \times 10^6$ mol/km^2/yr) is on the low end of the range for volcanic rivers ($1.35–3.29 \times 10^6$ mol/km^2/yr).

The weathering carbon export flux (i.e., alkalinity flux derived from silicate alteration) from the Philippines is $3.89 \pm 0.21 \times 10^6$ mol/km^2/yr weighted over both volcanic and ophiolitic regions. In volcanic regions, the export flux is $3.58 \pm 0.23 \times 10^6$ mol/km^2/yr, and in ophiolitic regions it is $5.99 \pm 0.64 \times 10^6$ mol/km^2/yr. These values are on the high end of atmospheric carbon export fluxes reported globally (Table 6). Importantly, these values are significantly higher than the global average values for export fluxes in tropical arcs, reported in Dessert et al. (2003) as 1.6×10^6 mol/km^2/yr. If our values are typical for fluxes from tropical volcanic arcs, it would appear that current estimates of the magnitude of weathering carbon fluxes from mafic and intermediate lithologies in tropical arc terranes are too low.

5. IMPLICATIONS FOR GLOBAL CO_2 EXPORT

In order to extrapolate our findings to other volcanic arcs in the tropics, we express the total export fluxes from the LVA and BVA as a function of arc length. We then assess the total length of volcanic arcs in the tropics (within 20 degrees of the Equator) and calculate the total fluxes expected from these arcs, assuming the fluxes we calculate for Luzon are representative of all tropical arcs. The length

Table 6
Comparison of carbon export fluxes, silicate cation weathering fluxes and silicate chemical weathering fluxes between different regions of the world.

River name	Country/ region	Lithology	Area (km^2)	Runoff (mm/yr)	Silicate weathering carbon export flux[a] (10^6 mol/km^2/yr)	Silicate cation weathering flux[b] (t/km^2/yr)	Silicate chemical weathering rate[c] (t/km^2/yr)	Source
Columbia Plateau	USA	Basalt		1053	0.37	7.7	24	a
Deccan Traps	India	Basalt		463	1.26	25	37	a
Hawaii	USA	Basalt		1612	0.66	12	34	a
Java	Indonesia	Basalt		4052	6.41	152	342	a
Massif Central	France	Basalt		406	0.30	5.6	13	a
Mt. Cameroon	Cameroon	Basalt		2120	3.44			a
Parana Traps	Brazil	Basalt		1020	0.82	21	60	a
La Reunion	La Reunion	Basalt		2433	2.26	48	106	a
Sao Miguel	Azores	Basalt		734	0.56	13	35	a
Iceland	Iceland	Basalt		2432	1.11	21	58	b
Siberian Traps	Central S	Basalt	700,000		0.1–0.3	5.7–6.1		h
Baltic Shield	NW Russia	Basalt		300–700		2.3	3.6	i
Irrawady	Myanmar	Mixed	410,000	1185	2.03	42	72	e
Brahmaputra	S Asia	Mixed	580,000	879	0.15	2.6	10	e
Ganges	S Asia	Mixed	1,050,000	470	0.45	7.9	14	e
Orinoco	S America	Mixed	1,100,000	1032	0.07	2.3	10	e
Nelson	Canada	Mixed	1,132,000	79	0.04	0.8	1.2	e
Mississippi	USA	Mixed	2,980,000	195	0.07	1.7	3.8	e
Ob	Siberia	Mixed	2,990,000	135	0.02	0.3	0.8	e
Congo-Zaire	W Africa	Mixed	3,698,000	324	0.05	0.8	4.2	e
Amazon	S America	Mixed	6,112,000	1078	0.05	2.2	13	e
Haut Glacier d'Arolla	Switzerland	Mixed	12	2009	0.002	13	18	g
Zambales/ Angat	Philippines	Ultramafic	1813	2539	6.07	100	192	f
Waitara	New Zealand	Volcanic	705		0.852[d]		113	c
Manganui, ds	New Zealand	Volcanic	200		2.39[d]		240	c
Kamchatka River, outlet	Russia	Volcanic	45,600	520	0.46[e]	8.03[e]	20.55[e]	d
Volcanic, all	Philippines	Volcanic	6236	2106	3.58	116	225	f

Sources: a, Dessert et al. (2003); b, Gislason et al. (1996); c, Goldsmith et al. (2008); d, Dessert et al. (2009); e, Gaillardet et al. (1999); f, this study; g, Sharp et al. (1995); h, Pokrovsky et al. (2005); i, Zakharova et al. (2005).

[a] Total bicarbonate flux, also called "carbon consumption" in published studies.

[b] Silicate cation weathering flux = Na* + K* + Ca* + Mg*.

[c] Silicate chemical weathering rate = Na* + K* + Ca* + Mg* + SiO_2.

[d] Carbon export flux calculated as twice the silica flux, as proposed by Edmond and Huh (1997).

[e] These values refer to low-temperature weathering only.

of arc studied in this paper is around 530 km. The segment of the LVA studied here is approximately 250 km long and the segment of the BVA studied is approximately 280 km long. We use values from von Huene and Scholl (1991) for length of arcs in the tropics. We adjusted the values given by von Huene and Scholl (1991) if a substantial part of an arc lies outside of the tropics, such as the Tonga and Mariana trenches. We also modified the lengths reported for the trenches surrounding the Philippine archipelago and for the Andaman-Sunda-Java trenches, since we were unable to verify the lengths given by von Huene and Scholl (1991). According to these calculations, volcanic arcs in the tropics stretch for 16,600 km.

The total weathering carbon export flux from the studied watersheds is 28×10^9 mol/yr, or 54×10^6 mol/km of arc length. Extrapolating this to the 16,600 km of volcanic arcs in the tropics, the total weathering carbon export flux from these systems is on the order of 0.9×10^{12} mol/yr. These calculations are subject to considerable uncertainty (e.g., uncertainty in the exact length of arcs in the tropics, inclusion of non-volcanic regions and/or exclusion of volcanoes, variable width/length ratios of arcs) and should be regarded as order of magnitude calculations only.

The weathering carbon export fluxes presented above represent about 10% of the global export of carbon by silicate weathering (Gaillardet et al., 1999). Because the composition of the cation flux is heavily weighted toward Ca + Mg, the long term sequestration potential of this flux is even greater than 10% of the global total (France-Lanord and Derry, 1997), although at present it is difficult to scale this with precision. As defined here the tropical volcanic arcs correspond to ~1% of the exorheic drainage area worldwide (Syvitski et al., 2005). Put another way, a fraction, perhaps as much as 15–20%, of all atmospheric carbon ultimately sequestered by silicate weathering may be processed through an area corresponding to ~1% of Earth's surface.

6. CONCLUSIONS

We initiated this study to test the hypothesis that chemical erosion rates in tectonically active, tropical volcanic arc terrains are very high. The data support this hypothesis; the silicate-weathering derived bicarbonate and cation fluxes and associated potential sequestration of atmospheric CO_2 are among the highest yet reported from any environment in the world. We found the highest area-normalized cation weathering fluxes in streams draining the lahar-dominated flanks of Mt. Pinatubo, and the lowest area-normalized cation weathering fluxes in Quezon, where volcanism ceased during the Pleistocene, and in Camarines. It is worth noting that even if these regions have the lowest weathering rates in this study, they still have some of the highest reported weathering rates in the world. Weathering rates in ultramafic rocks on Luzon are comparable to rates measured for low-temperature weathering rates in volcanic rocks, although the chemical composition differs.

We estimate that hydrothermal activity supplies around 10% of the dissolved cation load to streams on Luzon. This activity is restricted to areas surrounding known active volcanic centers. The estimate of the magnitude of hydrothermal contribution is subject to uncertainty, mainly because of the uncertainties in the composition of the hydrothermal end-member fluids, but because the total hydrothermal contribution is ca. 10% the uncertainties do not have a large impact on the overall flux estimate.

Extrapolating our findings to the entire length of volcanic arcs in the tropics yields a total weathering carbon export flux from tropical arcs of 0.9×10^{12} mol/yr. These values agree broadly with the values for global silicate weathering carbon export fluxes estimated by Gaillardet et al. (1999) and Dessert et al. (2003). Furthermore, we estimate that volcanic arcs in the tropics, while areally small, process around 10% of all atmospheric carbon exported by silicate weathering worldwide. Chemical weathering of volcanic arcs in the tropics thus has a markedly disproportionate impact on the long-term carbon cycle, an impact that exceeds by an order of magnitude the expected impact based on areal extent alone.

ACKNOWLEDGMENTS

First of all, we thank our drivers and field assistants on Luzon: William Tamayo, Gerald Quina, Gerardo Sumat, Cherisse Ferrer, Engielle Mae Paguican, Margaret Grace Honrado and Maria Gracia Collantes – this work would not have been possible without their professional, cheerful and enthusiastic support. PHIVOLCS provided housing and logistical support in Manila and Legazpi City, for which we are grateful. Adam Goss and Raymond Maximo introduced H.H.S. and L.A.D. to Philippine colleagues. Kathy Milidakis at BU is thanked for her help with sample analysis. Financial support from the following sources is gratefully acknowledged: NSF (SGER Grant # 0738828); BEB small grants in 2006 and 2007, Cornell University Graduate School Research Travel Grant and a semester-long ConocoPhillips Fellowship for H.H.S. Detailed and thoughtful reviews from Oleg Pokrovsky, Albert Galy and an anonymous reviewer greatly improved the quality of this paper.

APPENDIX 1. SENSITIVITY ANALYSIS FOR SOLUTE SOURCE ALLOCATIONS

To estimate the impact of variability in chemical ratios used to calculate sources of solutes (see Section 4.3, "Sources of solutes"), a sensitivity analysis was performed. The range of plausible values for element ratios in the relevant end-members (rainfall, hydrothermal fluids representative of high-temperature weathering) and the range of possible values for $[Cl^-]$ in rainfall were identified from literature data. Twenty-seven scenarios were constructed from all possible combinations of smallest, average and highest values for the three variables (element ratios in rainfall, element ratios in hydrothermal fluids and Cl-content of rainfall). For each scenario, the percentage contribution of each source (precipitation, high-temperature weathering and low-temperature weathering) was calculated for each stream. These values were then aggregated into an average (volcanic vs. ophiolite streams) percent contribution from each source for each solute within each scenario. Finally, the average percent contributions of each source to each solute from each of the 27 scenarios were compiled and

the CV calculated for all solutes and sources. The results are discussed in terms of CV, to emphasize not the absolute average percentage of a given solute deriving from a given source but to emphasize the variability of the possible results as a function of differences in input parameters.

Depending on what Cl-concentration is assumed for rainfall, the number of streams that have modeled contribution of high-T weathering products increases from 24 through 29 to 40, out of 65 streams in volcanic regions.

The percent contribution of precipitation to the solute load, especially to K-contents, is more sensitive to changes in the input parameters than either high-T weathering or low-T weathering. The average contribution of rainfall to the solute load in volcanic regions is 27% of Na, 10% of K, 6% of Mg and 1% of Ca. The CV of %Ca and %K in volcanic regions is high, around 70%, but since the contribution of rainfall to both K and especially Ca is small, the large CV does not impact weathering flux calculations significantly. In ophiolites, a significant fraction of both Na and K are derived from precipitation (average of 33% for Na and 41% for K) whereas Ca and Mg are overwhelmingly sourced from low-T weathering. The variability in %Na from rainfall in ophiolites is small, around 10%, whereas the variability in %K from rainfall is around 50%. K constitutes a very small part of the cation flux in ophiolites and the high CV leads to trivial differences in the allocation of solutes to low-T weathering in ophiolites. %Ca from rainfall in ophiolites is even higher, 70%, but in general, Ca is only to a small degree sourced from rainfall and just like with K, the high CV results in a trivial impact on low-T weathering fluxes from ophiolites.

In volcanic regions, the CV of contribution of low-temperature weathering products to the total cation load is modest for Na and K (6% and 10%, respectively) and very low for Ca and Mg (2%). This indicates that our results for low-T weathering fluxes are very robust and insensitive to the choice of input parameters when solutes are allocated to sources. A similar result is obtained for ophiolites, where the CV of low-T weathering products to the total cation load is >1% for Ca and Mg, 5% for Na and 35% for K. Since K is hardly present in ophiolite waters and the high CV for %K from low-T weathering is therefore of trivial importance.

High-temperature is assumed to only occur in volcanic regions. CV of the average contribution of high-T fluids to the total cation chemical flux is on the order of 20% (16% for K and Na, 20% for Ca and 22% for Mg). The contribution of high-T fluids to the total cation load of volcanic streams ranges from an average of 8% for Na to an average of 16% for K, and a CV of 20% thus has only a minor impact on the overall calculated high-T contribution to weathering in the Philippines.

Overall, these results suggest that our conclusions about low-temperature weathering fluxes from our study region are reasonably insensitive to variability in the magnitude of key parameters used to allocate solutes to their sources. The main exception is K, which is mainly sensitive to variations in K/Cl in rainfall. K is a minor component of river waters in ophiolite regions and constitutes on average less than 10% of the cation load of rivers in volcanic regions; the high sensitivity of this solute to model parameters is therefore of little consequence for our results of low-T weathering fluxes. The same may be said for high-temperature weathering, which is included in the final silicate weathering flux in this paper.

APPENDIX A. SUPPLEMENTARY DATA

Supplementary data associated with this article can be found, in the online version, at doi:10.1016/j.gca.2010.11.014.

REFERENCES

Andal E. S., Yumul G. P., Listanco E. L., Tamayo R. A., Dimalanta C. B. and Ishii T. (2005) Characterization of the Pleistocene Volcanic Chain of the Bicol Arc, Philippines: implications for geohazard assessment. *Terr. Atmos. Ocean. Sci.* **16**, 865–883.

Andal E.S. (2002) Geological and geochemical characterization of the Plio-Pleistocene to recent volcanic rocks of the southeastern Luzon Volcanic Arc Chain: implications to arc evolution. M.Sc. thesis, University of the Philippines.

Anonymous (1963) *Geological Map of the Philippines*. Department of Agriculture and Natural Resorces Bureau of Mines, Manila.

Arcilla C. A., Ruelo H. B. and Umbal J. (1989) The Angat ophiolite, Luzon, Philippines: lithology, structure, and problems in age interpretation. *Tectonophysics* **168**, 127–135.

Bachman S. B., Lewis S. D. and Schweller W. J. (1983) Evolution of a forearc basin, Luzon Central Valley, Philippines. *AAPG Bull.* **67**, 1143–1162.

Baltasar A. J. (1980) *Interpretations of the Water and Gas Chemistry from Three Geothermal Areas in the Philippines – Manito in Albay*. United Nations University, Biliran Island and Tongonan in Leyte, Orkustofnun.

Bethke C. (2007) *The Geochemist's Workbench. Hydrogeology Program*. University of Illinois.

Bevington P. R. and Robinson D. K. (2002) *Data Reduction and Error Analysis for the Physical Sciences*, third ed. McGraw-Hill, New York.

Castillo P. R. and Newhall C. G. (2004) Geochemical constraints on possible subduction components in Lavas of Mayon and Taal Volcanoes, Southern Luzon, Philippines. *J. Petrol.* **45**, 1089–1108.

Das A., Krishnaswami S., Sarin M. M. and Pande K. (2005) Chemical weathering in the Krishna Basin and Western Ghats of the Deccan Traps, India: rates of basalt weathering and their controls. *Geochim. Cosmochim. Acta* **69**, 2067–2084.

Defant M. J., Jacques D., Maury R. C., De Boer D. and Joron J. (1989) Geochemistry and tectonic setting of the Luzon arc, Philippines. *Geol. Soc. Am. Bull.* **101**, 663–672.

Delmelle P., Kusakabe M., Bernard A., Fischer T., de Brouwer S. and del Mundo E. (1998) Geochemical and isotopic evidence for seawater contamination of the hydrothermal system of Taal Volcano, Luzon, the Philippines. *Bull. Volcanol.* **59**, 562–576.

Derry L. A., Kurtz A. C., Ziegler K. and Chadwick O. A. (2005) Biological control of terrestrial silica cycling and export fluxes to watersheds. *Nature* **433**, 728–731.

Dessert C., Dupre B., Gaillardet J., Francois L. M. and Allegre C. J. (2003) Basalt weathering laws and the impact of basalt weathering on the global carbon cycle. *Chem. Geol.* **202**, 257–273.

Dessert C., Gaillardet J., Dupre B., Schott J. and Pokrovsky O. S. (2009) Fluxes of high- versus low-temperature water–rock interactions in aerial volcanic areas: example from the Kam-

chatka Peninsula, Russia. *Geochim. Cosmochim. Acta* **73**, 148–169.

DuFrane S. A., Asmerom Y., Mukasa S. B., Morris J. D. and Dreyer B. M. (2006) Subduction and melting processes inferred from U-series, Sr–Nd–Pb isotope, and trace element data, Bicol and Bataan arcs, Philippines. *Geochim. Cosmochim. Acta* **70**, 3401–3420.

Dyer S. D., Peng C., McAvoy D. C., Fendinger N. J., Masscheleyn P., Castillo L. V. and Lim J. M. U. (2003) The influence of untreated wastewater to aquatic communities in the Balatuin River, the Philippines. *Chemosphere* **52**, 43–53.

Edmond J. M. and Huh Y. (1997) Chemical weathering yields from basement and orogenic terrains in hot and cold climates. In *Tectonic Uplift and Climate Change*. Plenum Press, New York, pp. 330–351.

Eklund T. J., McDowell W. H. and Pringle C. M. (1997) Seasonal variation of tropical precipitation chemistry: La Selva, Costa Rica. *Atmos. Environ.* **31**, 3903–3910.

Encarnación J. P., Mukasa S. B. and Obille, Jr., E. C. (1993) Zircon U–Pb geochronology of the Zambales and Angat Ophiolites, Luzon, Philippines: evidence for an Eocene Arc-Back Arc Pair. *J. Geophys. Res.* **98**(B11), 19,991–20,004.

ESRI (2009) ArcGIS – The Complete Geographic Information System [online]. Redlands: ESRI. Available from: <http://www.esri.com/software/arcgis/index.html> (accessed April 2, 2010).

Evans C. A., Casteneda G. and Franco H. (1991) Geochemical complexities preserved in the volcanic rocks of the Zambales ophiolite, Philippines. *J. Geophys. Res.* **96**(B10), 16251–16262.

Evans M. J., Derry L. A., Anderson S. P. and France-Lanord C. (2001) Hydrothermal source of radiogenic Sr to Himalayan rivers. *Geology* **29**, 803–806.

Evans M. J., Derry L. A. and France-Lanord C. (2004) Geothermal fluxes of alkalinity in the Narayani river system of central Nepal. *Geochem. Geophys. Geosys.* **5**, Q08011.

Förster H., Oles D., Knittel U., Defant M. J. and Torres R. C. (1990) The Macolod Corridor: a rift crossing the Philippine island arc. *Tectonophysics* **183**, 265–271.

France-Lanord C. and Derry L. A. (1997) Organic carbon burial forcing of the carbon cycle from Himalayan erosion. *Nature* **390**, 65–67.

Fujita S., Takahashi A., Weng J., Huang L., Kim H., Li C., Huang T. C. and Jeng F. (2000) Precipitation chemistry in East Asia. *Atmos. Environ.* **34**, 525–537.

Gaillardet J., Dupre B., Louvat P. and Allegre C. J. (1999) Global silicate weathering and CO_2 consumption rates deduced from the chemistry of large rivers. *Chem. Geol.* **159**, 3–30.

Gaillardet J., Millot R. and Dupré B. (2003) Chemical denudation rates of the western Canadian orogenic belt: the Stikine terrane. *Chem. Geol.* **201**, 257–279.

Gislason S. R., Arnorsson S. and Armannsson H. (1996) Chemical weathering of basalt in Southwest Iceland; effects of runoff, age of rocks and vegetative/glacial cover. *Am. J. Sci.* **296**, 837–907.

Goldsmith S. T., Carey A. E., Lyons W. B. and Hicks D. M. (2008) Geochemical fluxes and weathering of volcanic terrains on high standing islands: Taranaki and Manawatu-Wanganui regions of New Zealand. *Geochim. Cosmochim. Acta* **72**, 2248–2267.

Goldsmith S. T., Carey A. E., Johnson B. M., Welch S. A., Lyons W. B., McDowell W. H. and Pigott J. S. (2010) Stream geochemistry, chemical weathering and CO_2 consumption potential of andesitic terrains, Dominica, Lesser Antilles. *Geochim. Cosmochim. Acta* **74**, 85–103.

Goldstein S. J. and Jacobsen S. B. (1987) The Nd and Sr isotopic systematics of river-water dissolved material – implications for the sources of Nd and Sr in seawater. *Chem. Geol.* **66**, 245–272.

Hawkins J. and Evans C. (1983) Geology of the Zambales Range, Luzon, Philippine Islands: ophiolite derived from an island arc-back-arc pair. In *The Tectonics and Geologic Evolution of Southeast Asian Seas and Islands, Part 2, AGU Geophys. Mono.* **27** (ed. D. E. Hayes), pp 124–138.

Kastner T. (2009) Trajectories in human domination of ecosystems: human appropriation of net primary production in the Philippines during the 20th century. *Ecol. Econ.* **69**, 260–269.

Knittel-Weber C. and Knittel U. (1990) Petrology and genesis of the volcanic rocks on the eastern flank of Mount Malinao, Bicol arc (southern Luzon, Philippines). *J. SE Asian Earth* **4**, 267–280.

Ku Y., Chen C., Song S., Iizuka Y. and Shen J. J. (2009) A 2 Ma record of explosive volcanism in southwestern Luzon: implications for the timing of subducted slab steepening. *Geochem. Geophys. Geosys.* **10**, Q06017.

Kyoung Lee B., Hee Hong S. and Soo Lee D. (2000) Chemical composition of precipitation and wet deposition of major ions on the Korean peninsula. *Atmos. Environ.* **34**, 563–575.

Liu Z., Zhao Y., Colin C., Siringan F. P. and Wu Q. (2009) Chemical weathering in Luzon, Philippines from clay mineralogy and major-element geochemistry of river sediments. *Appl. Geochem.* **24**, 2195–2205.

Louvat P. and Allegre C. J. (1998) Riverine erosion rates on Sao Miguel volcanic island, Azores archipelago. *Chem. Geol.* **148**, 177–200.

Louvat P. and Allegre C. J. (1997) Present denudation rates on the island of Reunion determined by river geochemistry: basalt weathering and mass budget between chemical and mechanical erosions. *Geochim. Cosmochim. Acta* **61**, 3645–3669.

Lyons W. B., Carey A. E., Hicks D. M. and Nezat C. A. (2005) Chemical weathering in high-sediment-yielding watersheds, New Zealand. *J. Geophys. Res.* **110**, F01008.

McArthur J., Howarth R. J. and Bailey T. R. (2001) Strontium isotope stratigraphy: LOWESS version 3: best fit to the marine Sr-isotope curve for 0–509 Ma and accompanying look-up table for deriving numerical age. *J. Geol.* **109**, 155–170.

McDermott F., Delfin, Jr., F., Defant M., Turner S. and Maury R. (2005) The petrogenesis of volcanics from Mt. Bulusan and Mt. Mayon in the Bicol arc, the Philippines. *Contrib. Mineral. Petrol.* **150**, 652–670.

Meybeck M. and Ragu A. (1995) *GEMS/Water Contribution to the Global Register of River Inputs (GLORI). Provisional Final Report*. UNEP/WHO/UNESCO, Geneva.

Meybeck M. (1987) Global chemical weathering of surficial rocks estimated from river dissolved loads. *Am. J. Sci.* **287**, 401–428.

Milliman J. D., Farnsworth K. L. and Albertin C. S. (1999) Flux and fate of fluvial sediments leaving large islands in the East Indies. *J. Sea Res.* **41**, 97–107.

Milliman J. D. and Syvitski J. P. M. (1992) Geomorphic/tectonic control of sediment discharge to the ocean; the importance of small mountainous rivers. *J. Geol.* **100**, 525–544.

Montgomery D. R., Panfil M. S. and Hayes S. K. (1999) Channel-bed mobility response to extreme sediment loading at Mount Pinatubo. *Geology* **27**, 271–274.

Mortlock R. and Froelich P. (1989) A simple method for the rapid determination of biogenic opal in pelagic marine sediments. *Deep-Sea Res.* **36**, 1415–1426.

Neal C. and Shand P. (2002) Spring and surface water quality of the Cyprus ophiolites. *Hydrol. Earth Syst. Sci.* **6**, 797–817.

Oksanen J. and Sarjakoski T. (2005) Error propagation analysis of DEM-based drainage basin delineation. *Int. J. Remote Sens.* **26**, 3085–3102.

Ozawa A., Tagami T., Listanco E. L., Arpa C. B. and Sudo M. (2004) Initiation and propagation of subduction along the

Philippine Trench: evidence from the temporal and spatial distribution of volcanoes. *J. Asian Earth Sci.* **23**, 105–111.

Pallister J. S., Hoblitt R. P. and Reyes A. G. (1992) A basalt trigger for the 1991 eruptions of Pinatubo Volcano?. *Nature* **356** 426–428.

Pokrovsky O. S., Schott J., Kudryavtzev D. I. and Dupre B. (2005) Basalt weathering in Central Siberia under permafrost conditions. *Geochim. Cosmochim. Acta* **69**, 5659–5680.

Rad S., Louvat P., Gorge C., Gaillardet J. and Allegre C. J. (2006) River dissolved and solid loads in the Lesser Antilles: new insight into basalt weathering processes. *J. Geochem. Explor.* **88**, 308–312.

Reuter H. I., Nelson A. and Jarvis A. (2007) An evaluation of void-filling interpolation methods for SRTM – data. *Int. J. Geogr. Inf. Sci.* **21**, 983–1008.

SAS (2009) *JMP, Version 8.0*. SAS Institute Inc., Cary, NC, USA.

Schlesinger W. (1997) *Biogeochemistry: an Analysis of Global Change*, second ed. Academic Press, San Diego, Calif.

Schellart W. and Rawlinson N. (2010) Convergent plate margin dynamics: new perspectives from structural geology, geophysics and geodynamic modelling. *Tectonophysics* **483**, 4–19.

Sharp M., Tranter M., Brown G. H. and Skidmore M. (1995) Rates of chemical denudation and CO_2 drawdown in a glacier-covered alpine catchment. *Geology* **23**, 61–64.

Stimac J. A., Goff F., Counce D., Larocque A. C. L., Hilton D. R. and Morgenstern U. (2004) The crater lake and hydrothermal system of Mount Pinatubo, Philippines: evolution in the decade after eruption. *Bull. Volcanol.* **66**, 149–167.

Syvitski J. P. M., Vorosmarty C. J., Kettner A. J. and Green P. (2005) Impact of humans on the flux of terrestrial sediment to the Global Coastal Ocean. *Science* **308**, 376–380.

von Huene R. and Scholl D. W. (1991) Observations at convergent margins concerning sediment subduction, subduction erosion, and the growth of continental-crust. *Rev. Geophys.* **29**, 279–316.

Waterloo M. J., Schelleken J., Bruijnzeel L. A., Vugts H. F., Assenberg P. N. and Rawaqa T. T. (1997) Chemistry of bulk precipitation in Southwestern Viti Levu, Fiji. *J. Trop. Ecol.* **13**, 427–447.

Wolff-Boenisch D., Gabet E. J., Burbank D. W., Langner H. and Putkonen J. (2009) Spatial variations in chemical weathering and CO_2 consumption in Nepalese High Himalayan catchments during the monsoon season. *Geochim. Cosmochim. Acta* **73**, 3148–3170.

Yumul G. P., Dimalanta C. B. and Jumawan F. T. (2000) Geology of the southern Zambales ophiolite Complex, Luzon, Philippines. *Isl. Arc* **9**, 542–555.

Zakharova E. A., Pokrovsky O. S., Dupre B. and Zaslavskaya M. B. (2005) Chemical weathering of silicate rocks in Aldan Shield and Baikal Uplift: insights from long-term seasonal measurements of solute fluxes in rivers. *Chem. Geol.* **214**, 223–248.

Associate editor: Jérôme Gaillardet